

1 **Macroscopic to microscopic scales of particle dosimetry: from source to fate in the body**

2 Paul A. Solomon¹, Peter Gehr², Deborah H. Bennett³, Robert F. Phalen⁴, Loyda B. Méndez^{4,5,6}, Barbara
3 Rothen-Rutishauser⁷, Martin Clift², Christina Brandenberger², Christian Mühlfeld⁸

4

5 1. U.S. Environmental Protection Agency, Office of Research and Development, National Exposure
6 Research Laboratory, Las Vegas, NV, USA.

7 2. Institute of Anatomy, University of Bern, Bern, Switzerland

8 3. Department of Public Health Sciences, School of Medicine, University of California, Davis, CA, USA

9 4. Department of Medicine, School of Medicine, University of California, Irvine, CA, USA,

10 5. Microbiology and Molecular Genetics, School of Biological Sciences, University of California, Irvine,
11 CA, USA

12 6. Pacific Southwest Regional Center of Excellence, Irvine, CA, USA

13 7. Bio-Nanomaterials, Adolphe Merkle Institute, University of Fribourg, Marly, Switzerland

14 8. Institute of Functional and Applied Anatomy, Hannover Medical School, Hannover, Germany

15

16 **Abstract**

17 Additional perspective with regards to particle dosimetry is achieved by exploring dosimetry across a
18 range of scales from macroscopic-to-microscopic in scope. Typically, one thinks of dosimetry as what
19 happens when a particle is inhaled and where it is deposited and how it is cleared from the body.
20 However, this paper shows a much more complicated picture starting with emissions sources, showing
21 how the source-to-intake fraction (iF) can be used to estimate changes in the inhaled dose due to
22 changes in emissions and then ending with particle-liquid, particle-cellular and subcellular interactions
23 and movement of ultrafine particles across the lung-blood barrier. These latter issues begin to suggest
24 mechanisms that can lead to adverse health effects the former can provide guidance to policy decisions
25 designed to reduce the health impact of atmospheric particles. The importance of ultrafine particles, their
26 ability to translocate to other parts of the body, and the potential impact of these particles has advanced
27 significantly over the last decade, including studies that show the movement of ultrafine particles along
28 the olfactory nerves in the nose with direct transport to the brain; the neurological effects of which are still
29 unknown. Incremental advancements continue with regards to understanding particle deposition,
30 including regional and local deposition (including hot spots), and clearance and the factors that affect
31 these variables, in part due to the development and implementation of computational fluid dynamics
32 (CFD) models and digital imaging of the lungs. CFD modeling will continue to provide new information for
33 reducing uncertainty in dosimetric calculations. We better understand today how a number of diseases
34 may develop based on the fate of particles after deposition in the lung and how changes in source

35 emissions might impact that dose. However, a number of uncertainties remain some of which can be
36 reduced by addressing the research needs stated in this paper.

37

38 **Introduction**

39 Leonardo da Vinci (1452-1519) warned readers in his Anatomical Atlas that “dust is harmful” (Gehr et al.
40 2010), and Paracelsus (1493—1541) added “The right dose differentiates a poison from a remedy” (Gallo
41 2008). This paper on particle dosimetry integrates and updates these concepts in the interest of reducing
42 the adverse health effects of modern air pollution. This paper also addresses, in part, one of the policy-
43 relevant Science Questions that formed the basis of the 2010 international conference “Air Pollution and
44 Health: Bridging the Gap between Sources and Health Outcomes”¹ (Solomon et al. 2011). Specifically
45 this paper addresses Science Question 4 “*What advances have been made in understanding the*
46 *relationships between exposure, both spatially and temporally, and estimates of dose that tie to health*
47 *outcomes?*”

48 Current research continues to show significant associations of fine particles with adverse health effects
49 (Brook et al. 2010, He et al. 2010, Pope et al. 1995, 2009, Puett et al. 2009). Reducing the adverse
50 health effects from air pollution requires knowledge across the source-to-health effects paradigm: source
51 – atmospheric sciences – exposure – dose – health effect (NRC 1998; Mauderly et al. 2011, this issue;
52 Solomon et al. 2011). Linking sources to adverse health effects is complicated due to the many factors,
53 such as, source variability, the complex and changing nature of pollutants in air (e.g., see Seinfeld and
54 Pandis 1998; Finlayson-Pitts and Pitts 2000) as well as component toxicity, anatomical and physiological
55 factors, susceptibility and vulnerabilities of the target to pollutants, and confounding factors (2009a (Table
56 8-1); Sheppard et al. 2011, this issue; Mauderly et al. 2011, this issue; O’Neil et al. 2011, this issue).

57 Dosimetry research involves a broad understanding of source-to-dose relationships, essentially the first
58 half of the source to health effects continuum. Dosimetric research encompasses a variety of *scales*
59 ranging from the *macroscopic* to the *microscopic*. As well, the dose of the causal agent(s) received and
60 retained are key parameters regarding the impact of an air pollutant that results in an adverse health
61 effect.

62 At the macro-scale, the *intake fraction*, *iF*, is a parameter that provides an estimate of the amount of a
63 pollutant that is inhaled (not deposited nor retained), relative to the amount emitted into the environment
64 from a specified source or source category. The *iF* begins to provide an understanding and quantification
65 of pollutant source-to-intake relationships. The *iF* precedes the deposition in the body of an inhaled air

¹ American Association for Aerosol Research held in San Diego, CA March 22-26, 2010,
<http://aar.2010specialty.org/> (Solomon et al. 2011).

66 pollutant, which is an important parameter for dosimetry considerations, since the respiratory tract (RT) is
67 the dominant exposure route.

68 Moving from the macro- towards the micro-scale, this paper next considers the fate of a pollutant during
69 and just after inhalation. The inhalability, more specifically the *inhalable fraction* (η_i), describes the
70 sampling efficiency of the nose and/or mouth. The η_i is the ratio of pollutant concentration in the
71 breathing zone (the immediate vicinity of the face) to the concentration that is inspired and enters the
72 *extrathoracic* (ET) airways. The inhalation of particles into the nose or mouth follows the airflow where
73 deposition may occur in any of the major regions of the RT shown schematically in Figure 1a and with
74 micrographs for the gas exchange region of the lungs in Figure 1b. The three main regions include: the
75 ET, *tracheobronchial* (TB), and the *alveolar-interstitial* (AI) regions. The particle deposition efficiencies in
76 each of the major RT regions have been modeled for adults and children breathing at various levels of
77 exertion (e.g. ICRP 1994; EPA 2009a) (e.g., Figure 2).

78 Following deposition within the RT, particles are subject to a variety of fates in the body. They may be
79 retained in the RT for times ranging from minutes (or less) to a lifetime depending on a number of factors
80 described later. Particles not retained in the lungs are removed or cleared by *mechanical processes*
81 (e.g., mucociliary activity, coughing, swallowing), by *phagocytosis* (engulfed by cells and then sometimes
82 digested), and by *translocation*, in which particles or their products move from the RT to other parts of the
83 body. Deposition and clearance phenomena also are individual- and species-dependent (EPA 2009a).

84 At the micro-scale, deposited particles interact with fluids and cells throughout the body. The interactions
85 are varied, and are the subject of ongoing research (Gehr et al. 2010). Interactions with fluids and cells in
86 the body include dissolution, transport within the fluids, uptake by cells and tissue elements, and other
87 physiologic phenomena. These interactions will largely determine the health-related consequences that
88 follow pollutant deposition and again are dependent on a number of factors. Recent research has
89 identified *ultrafine particles* (UF particles; generated by ambient air pollution sources and formed from gas
90 phase precursors in the atmosphere) with dimensions $\leq 0.1 \mu\text{m}$, and their intentionally engineered
91 counterparts, *nanoparticles* (NP), as having unique fates in the body and the potential to cause adverse
92 health effects (Wichmann et al. 2000; Renwick et al. 2004; Geiser et al. 2005; Schultz et al. 2005;
93 Oberdörster et al. 2005; de Haar et al. 2006; Donaldson et al. 2006; Kreyling et al. 2002, 2006a, 2006b).
94 Throughout this summary, the term UF particles will be used to refer to both UF particles resulting from air
95 pollution and nanoparticles that are intentionally engineered. UF particles can have access to the entire
96 RT and other organs of the body including the brain (see section, *Particle Translocation*), they likely have
97 the potential for producing greater adverse effects than would be predicted from their mass alone. Thus
98 particle number, composition, or surface area may be more important for dosimetric purposes
99 (Oberdörster 2010).

100 The dose *metric* (or indicator) refers to key pollutant properties that must be measurable, and have a
101 causal relationship to one or more biological responses (Phalen et al. 2010). The metric may have

102 physical and/or temporal properties. Also, the metric need not be causal for every exposed individual
103 (Phalen et al. 2010). Table 1 lists some known or proposed particle-related metrics relevant to the health
104 effects of inhaled air-pollutant particles. In the body, dose metrics differ for soluble versus insoluble
105 particles. For example, common metrics for soluble particles may include particle mass, composition, and
106 aerodynamic diameter (dae). For insoluble particles the metrics also might include surface area, particle
107 count, or other physical properties. Composition is usually a key metric for all air pollutants. All metrics
108 are likely important and should be considered in evaluating pollutants for potential adverse health effects.

109 Relevant biological targets include anatomical (e.g. a cell type, tissue, organ, or organ system) or
110 physiological effects, such as an essential biochemical process (e.g., lung surfactant synthesis) or a
111 system function (e.g., learning or memory).

112 This paper describes the current understanding of selected macro- and micro-scale phenomena related
113 to the adverse health effects of inhaled particles in human subjects, emphasizing current research in
114 dosimetry. *In-vitro* studies have their own set of challenges, and one of the greatest is relating or
115 extrapolating results from *in-vitro* experiments to humans (Gerde 2008), however a detailed discussion of
116 this is outside the scope of this paper. For brevity, details and examples of many other topics discussed
117 can be found in the references, which themselves provide only examples due to the vastness of the
118 applicable literature in this growing field.

119 **Source-to-Intake Relationships: Intake Fraction**

120 Determining source-to-intake relationships for air pollutants allows for an estimate of the relative intake of
121 a pollutant(s) to a population from a particular source category. One advantage is it allows for an
122 estimate of the relative decreases in exposure resulting from decreases in emissions from the subject
123 source category. A source-to-intake relationship takes into consideration the resulting concentrations
124 from a pollutant released into the environment, determines the exposure concentrations, and considering
125 breathing rate, estimates resulting intake to members of the population. A useful measure to estimate
126 source-to-intake relationships is the intake fraction (*iF*) (Bennett et al. 2002a). The *iF* is defined as the
127 integrated incremental intake of a pollutant, summed over all exposed individuals, and occurring over a
128 given exposure time, released from a specified source or source class, per unit of pollutant emitted. The
129 definition is expressed in the equation below:

130

$$131 \quad iF = \frac{\sum_{\text{people, time}} \text{intake of pollutant by an individual (mass)}}{\text{mass released into the environment (mass)}} \quad \text{eq. 1}$$

132

133 There are two dimensions over which the pollutant intake is summed, population and time. In actuality,
134 when a pollutant is released into the environment there is a distribution of individual exposures within the
135 exposed population. For transient release scenarios, *iF* is made dimensionless by dividing the time-
136 integrated intake by the total quantity released. For steady-state release and exposure conditions, *iF* is

137 the rate of intake divided by the rate of release, both using units expressed as mass per time. If the
138 compound is persistent in the environment, then the exposure that occurs over the duration of the
139 compound being present must be considered.

140 The *iF* allows different pollutant release scenarios to be considered, such as releases into the indoor
141 environment, from outdoor mobile sources, or from industrial facilities (Humbert et al. 2011). Various
142 environments to which the pollutant may be released also can be considered, such that one can
143 differentiate between urban and rural regions or indoor and outdoor. In the case of some chemical
144 pollutants, one may need to sum across multiple exposure pathways (i.e., considering inhalation,
145 ingestion, and dermal pathways) (Bennett et al. 2002b). For air pollutant regulation, *iF* primarily (or
146 exclusively) considers inhalation.

147 There are four attributes of the *iF* that further increases its usefulness. First, *iF* considers both the release
148 scenarios and fates of the pollutant in the environment (Bennett et al. 2002a;)). Second, *iF* can be
149 disaggregated to consider various populations (e.g., susceptible groups) that can then be summed to
150 equal the total *iF* (Tainio et al. 2009; Greco et al. 2007a; Zhou and Levy 2008; Ries et al. 2009; Marshall
151 and Behrentz 2005). Third, *iF* is compatible with dose-response calculations (Levy et al. 2009). Forth, *iF*
152 values can be calculated from models or from measured data (Bennett et al. 2002b, Tainio et al. 2009,
153 Greco et al. 2007a, 2007b, Zhou and Levy 2008, Levy et al. 2009, Hao et al. 2007, Heath et al. 2006,
154 Klepeis and Nazaroff 2006, Li and Hao 2003, Luo et al. 2010, Stevens et al. 2007, Wang et al. 2006; Ries
155 et al. 2009). While the *iF* value itself is a single, simple value, considerable complexity goes into the
156 calculation. When calculating *iF* values using a model, the concentration profile in the surrounding area
157 first needs to be determined. Dispersion models with varying levels of complexity have frequently been
158 used in calculations. The concentration profile is then overlaid with the population density to determine
159 the number of individuals exposed to the pollutant. This brings in the population density of the
160 surrounding area. Breathing rates then determine the actual intake, such that a total mass of particulate
161 matter inhaled can be determined.

162 In limited cases there is complete information on the total emissions of the compound into the
163 environment and sufficient measurements of resulting concentrations have been made such that one can
164 calculate an *iF* value solely from the measured data, without the use of models (Bennett 2002b and Ries
165 2009).

166 The resulting values are therefore subject to uncertainties resulting from model calculations and full
167 quantification of these uncertainties is beyond the scope of this paper. A recent review quantified model
168 uncertainties and found that variability in population density exceeded model uncertainties (Humbert
169 2011). The inclusion of the exposed population in the calculation makes *iF* values very useful for
170 comparing release scenarios, minimizes the impact of model uncertainties, and points out the need for
171 improved understanding of the exposed population.

172 Research communities can benefit from the numerous applications and models available in which the *iF*
173 can be obtained from and incorporated. Within the modeling community, *iF* can facilitate the evaluation of
174 models, both by comparing *iF* values calculated by models and through measured data (Bennett et al.
175 2002b) and by the comparing results between or among models. Another application is to generate
176 modeling results in one location and use those results in another location after making necessary
177 adjustments, such as for differences in population density (Stevens et al. 2007). This is useful when
178 there are limited available data, or limited resources, such that it would otherwise be difficult to conduct
179 an extensive model evaluation. Although *iF* values cannot be directly used in health assessments, values
180 can be combined with dose-response functions, allowing for comparative risk assessment or evaluation of
181 health-related damages from a release (Levy et al. 2009). The *iF* also is useful with a variety of tools
182 used in decision-making, such as risk management, life cycle assessment, emissions trading, sustainable
183 development, and policy development. Thus, *iF* modeling and the application of *iF* in models can assist in
184 evaluating new sources and for determining the most effective way to reduce sources (Heath et al. 2006;
185 Humbert et al. 2011).

186 When using models to calculate *iF* values, a wide range of models with varying levels of complexity have
187 been used by various researchers. The resulting values are therefore subject to uncertainties resulting
188 from model calculations and full quantification of these uncertainties is beyond the scope of this paper. A
189 recent review quantified model uncertainties and found that variability in population density exceeded
190 model uncertainties (Humbert 2011). The inclusion of the exposed population in the calculation makes *iF*
191 values very useful for comparing release scenarios, minimizes the impact of model uncertainties, and
192 points out the need for improved understanding of the exposed population.

193 Intake fraction values for PM emissions

194 A series of *iF* values calculated for PM_{2.5} emissions derived from power plants (Levy et al. 2009; Heath
195 et al. 2006; Wang et al. 2006; Hao et al. 2007; Li and Hao 2003), mobile sources (Greco et al. 2007a;
196 Zhou and Levy 2008; Stevens et al. 2007), area sources (Ries et al. 2009) and indoor sources; Klepeis
197 and Nazaroff 2006) are illustrated in Figure 3. In this figure, *iF* values span over three orders of
198 magnitude among emission sources, ranging from 0.1×10^{-6} to 3×10^{-3} , which is similar to *iF* values
199 calculated for various volatile and semi-volatile organic (VOC and SVOC, respectively) chemicals
200 (Bennett et al. 2002b), also plotted in Figure 3.

201 This extreme range highlights the importance of targeting emission reduction strategies on sources with
202 the highest intake fraction values. When *iF* is taken into account along with the magnitude of the source
203 and any potential differences in the relative toxicity between particle emissions from various sources,
204 regulators could likely develop strategies that could result in health improvements.

205 *iF* values resulting from power plants in Europe, the U.S., and China are shown towards the left side of
206 Figure 3. U.S. values were based on a comprehensive study of PM_{2.5} emissions from 407 power plants,

207 with exposures estimated using a source-receptor matrix (Levy et al. 2009). *iF* values from power plants
208 in Europe were obtained based on the average *iF* values calculated for different countries within Europe
209 (Tainio et al. 2009). *iF* values for China were calculated from power plants in Beijing (Hao et al. 2007)
210 and the Hunan Province (Li and Hao 2003). Similar *iF* values were observed between the US and Europe
211 but were slightly higher for China due to its higher population density (e.g., 84 per sq mile in the US
212 versus 365 in China; <http://www.infoplease.com/ipa/A0934666.html>). A value from a hypothetical small
213 distributed energy power plant (DE) in an urban area also is included (Heath et al. 2006).

214 For mobile sources, *iF* values were calculated for urban areas of Boston, MA (Greco et al. 2007a), urban
215 street canyons in New York City, NY (Zhou and Levy 2008), Hong Kong (Luo et al. 2010) and estimated
216 for Mexico City from these previous studies (Stevens et al. 2007). Additional *iF* values from mobile
217 sources are available for each county in the U.S. (Greco et al. 2007b), although these values may be an
218 underestimate due to lack of sufficient detail and modeling of near-road exposures. The variability in
219 values resulting from mobile source emissions among locations largely results from differences in
220 population density (e.g. Hong Kong) and/or high exposure levels (e.g. NY street canyons). An *iF* value for
221 school buses also has been calculated, including exposures to both people inside and outside the bus,
222 thereby resulting in a higher intake fraction value than for other mobile sources (Marshall and Behrentz
223 2005).

224 There are limited examples in the literature of *iF* values for specific area sources. *For example*, *iF* values
225 for woodsmoke emissions in Vancouver were calculated for a large wildfire (Ries et al. 2009). In this
226 example, levoglucosan, a unique marker for wood smoke was used to determine the portion of the
227 particulate matter that resulted from the wildfire, allowing the authors to determine the relationship
228 between measured concentrations and the source rate.

229 For indoor tobacco smoke, *iF* values were calculated for different scenarios in which individuals were in
230 the same room as the smoker, different room than the smoker, and also by varying the HVAC system
231 (Klepeis and Nazaroff 2006). The resulting *iF* values in the tobacco study were dependent on air
232 exchange rates and the location of people in relation to the source.

233 The *iF* is a simple, transparent, and comprehensive measure of the source-to-intake relationship. As
234 shown in Figure 3, the non-dimensionality of *iF* facilitates comparisons of values calculated from different
235 emission sources and it can be compared among investigators and modeling scenarios. It also is a
236 metric that can be calculated for any scenario and can be reported in addition to plots of concentration.
237 This highlights the utility of *iF* calculations in understanding source-to-intake relationships and in decision-
238 making policies for targeting emission reduction strategies that may have the greatest impact in protecting
239 public health.

240 **The Fate of Inhaled Particles in the Respiratory Tract**

241 Moving from the macroscopic view, and having an estimate of the fraction of air pollutants that can enter
242 the body (iF) this section considers the fate of inhaled atmospheric particles inside the body. The fate of
243 inhaled particles involves four general steps: deposition; clearance; translocation; and retention (EPA
244 2009a). *Deposition* occurs when inhaled particles contact the wall of an airway and can occur during
245 inhalation or exhalation. *Clearance* commonly refers to either removal of the particles from the respiratory
246 tract or from the entire body. *Translocation* refers to the extrapulmonary movement of particles from the
247 lungs to other locations in the body. *Retention* is simply what remains in the body at some post exposure
248 time, whether within the lung or elsewhere in the body. Chemical transformation of pollutants also occurs
249 in the body. Each step is dependent on a range of physical, chemical, and biological factors that include:
250 particle properties; exposure location; breathing patterns; and anatomical and physiological
251 characteristics of the exposed subjects such as disease states, body size, age, race, and gender.

252 Particle Deposition

253 An inhaled particle can deposit anywhere within the RT upon contacting a surface within the RT; it is
254 assumed that both bounce and re-entrainment are negligible. Within the RT, the AI region of the lungs
255 where gas exchange occurs is of interest due to its large internal surface area of about 150 m² and the
256 very thin air-blood tissue barrier of <1 μm in thickness over a large part of the lung's surface, which is
257 primarily located in the AI region (see Figure 1b) (Gehr *et al.* 1978).

258 Particle deposition occurs by several mechanisms in the RT as described below and depends strongly on
259 the size of the inhaled particle, the route of inhalation (nose versus mouth), the tidal volume (V_T), the
260 breathing frequency, RT disease, and the RT morphology (ICRP 1994; EPA 2009a). Physical exertion
261 and reflex-mediated bronchial caliber may be important in some exposure scenarios, for example rescue
262 operations. These factors can influence which deposition mechanisms are dominant within the different
263 regions of the RT (Figure 1). Biological factors depend on the mammalian species, size, status of
264 development and growth and health status, since they will affect lung structure and function, and thus,
265 particle deposition and subsequent fate.

266 Much is known about the deposition of inhaled “ideal” particles, i.e. smooth uncharged solid spheres with
267 unit density (1 gm/cm³). In the diameter range from 0.01 to 100 μm aerodynamic diameter (d_{ae}), the
268 particle mass, surface area, the number of particles of a given size in 1 μg of ideal particles as well as
269 how far an ideal particle of a given size will travel in a second in still air based on gravitational settling and
270 diffusion are well known Phalen *et al.* (2010). Such particle characteristics are used for dose calculations.
271 The major mechanisms for the deposition of particles in the RT include inertial impaction, gravitational
272 sedimentation, and Brownian diffusion (ICRP 1994; Brown *et al.* 2005; EPA 2009a). The first two
273 deposition mechanisms depend on the d_{ae} , which is the physical diameter of a sphere of standard density
274 that has the same gravitational terminal settling velocity as the particle in question. Aerodynamic
275 diameter is most applicable to particles larger than about 0.3 μm (EPA 2009a). Diffusion is

276 thermodynamically controlled, and it dominates the motion of particles less than a few tenths of
277 micrometer in physical diameter, where gravitational and inertial effects are usually negligible.

278 Within the RT, impaction is an efficient deposition mechanism for larger particles, occurring primarily in
279 areas with obstructions or sharp transitions, such as in the nasal turbinates, the larynx, and at airway
280 bifurcations, thus primarily in the ET and upper TB. Sedimentation probability is inversely proportional to
281 the airflow rate and is most important in the lower TB and AI regions, where airflow velocities are low and
282 distances to the walls of airways are small. Both impaction and sedimentation are important for particles
283 in the size range above $1 \mu\text{m } d_{ae}$ (EPA 2009a). Deposition due to diffusion is proportional to residence
284 times and proximity to airway walls, so it occurs effectively at low velocities and with turbulent flow. Thus
285 particles with diameters under $0.1 \mu\text{m } d_{ae}$ deposit most efficiently in the lower TB and AI regions.
286 Particles in this size range also tend to deposit due to diffusion in the ET and upper TB regions. Figures
287 2a and 2b illustrate typical deposition curves, including total deposition and deposition in the major RT
288 regions; the curves are for an adult male at rest and at a light exercise. The competing mechanisms of
289 impaction, diffusion, and sedimentation results in the typical U-shaped total RT deposition curves, with a
290 minimum in the range between 0.1 and $1 \mu\text{m } d_{ae}$, since particles in this size range are too small to be
291 efficiently impacted or undergo significant gravitational settling, and are too large to be strongly influenced
292 by diffusion. Total deposition approaches 100% for particles larger than about $10 \mu\text{m } d_{ae}$ and less than
293 $0.01 \mu\text{m}$ in diameter, due to the high efficiency of impaction and sedimentation, and diffusion,
294 respectively. Average curves are shown in Figure 2, but each individual has a unique particle deposition
295 pattern at any given time because of the complexity of the deposition process. Thus, caution must be
296 applied when using average curves for population or individual risk assessment purposes.

297 Respiratory tract disease, from the typical acute infections that adults get 1-3 times per year, to advanced
298 chronic obstructive pulmonary disease (COPD), can significantly influence particle deposition by altering
299 airway structure and ventilatory parameters (see EPA 1996, 2004 for original references). Changes in
300 disease states include differences in regional lung deposition, more heterogeneous deposition patterns,
301 greater deposition in the TB region, and a decrease in the AI deposition due to less particles reaching the
302 AI region. Total RT deposition is generally increased with increasing airway obstruction. Slower
303 clearance in COPD patients was observed by Scheuch et al. (2008), which may be limited to the larger
304 bronchial airways. However, Smaldone et al. (1993) and Brown et al. (2002) found normal clearance in
305 peripheral airways in COPD patients. Relative to healthy adults, individuals with COPD, in which a more
306 limited lung volume receives the total airflow, had a similar resting V_T and an increased breathing
307 frequency; thus a higher than normal tidal peak flow, minute ventilation, and average deposition rate of
308 particles, all suggesting higher doses for individuals with COPD (Bennett et al. 1997; Phalen et al. 2010;
309 EPA 1996, 2004, 2009a). Additional discussion on this topic can be found in Phalen et al. (2010) and
310 EPA (2009a) and references within these publications.

311 The complex morphology of the RT (e.g., bifurcations, bends, and other obstructions to airflow), in
312 conjunction with the several deposition mechanisms results in a strongly non-uniform distribution of
313 deposited particles. Particles greater than about $1 \mu\text{m } d_{ae}$ and UF particles deposit preferentially at
314 bifurcations, mainly on the carinal ridges, due to impaction and secondary flow patterns. These areas are
315 referred to as *hot spots* that result from high particle deposition in small areas (EPA 2009a; Kleinstreuer
316 and Zhang 2010; Phalen et al. 2006). The size of the hot spot area is referred to as the *patch size* by
317 dosimetry modelers. Hot spots are illustrated in Figure 4. In this figure, computational fluid dynamic
318 (CFD) simulations are used to model the deposition of UF (NP) particles and gases and micrometer sized
319 particles in the ET and upper TB (mouth to large bronchi).

320 Deposition enhancement factors (EFs) are used to quantify hot spot deposition dose enrichments. The
321 EF is defined as the ratio of particles deposited at the hot spot per unit surface area of epithelial cells
322 (e.g., a patch size of $0.1 \text{ mm} \times 0.1 \text{ mm}$) to the average deposition on the surrounding tissue (Kleinstreuer
323 and Zhang 2010; EPA 2009a; Balásházy et al. 1999, 2003). EFs, estimated from CFD modeling, are
324 shown as a function of patch size and particle diameter in Table 2, and as a function of ventilation rate (5
325 and 30 L/min) in Table 3 (Balásházy et al. 1999, 2003). In these examples, EFs range from less than 10
326 to about 400 times that of the surrounding epithelial surface. EFs up to 1,200 have been reported
327 (Farkas and Baláshazy 2008). Hot spots also bring up a unique challenge for cell culture studies with
328 respect to air pollutant dosing of the *in-vitro* system (Phalen et al. 2006). Should an average dose be
329 applied, the enhanced dose applied to the entire culture, or the enhanced dose just applied to a
330 reasonable patch sizes surrounded by cells in the culture with no dose?

331 Particle clearance

332 Clearance usually refers to the removal of deposited particles from the RT, whether removed from the
333 body or translocated to other parts of the body (e.g., through the respiratory epithelium) where they may
334 be subsequently removed from the body by other mechanisms. Clearance rate data for inhaled particles
335 from the RT are required in dosimetric calculations. The rates and mechanisms of particle clearance
336 depend on the size of the particle, where it has deposited, whether it is *soluble* or *insoluble*, health status
337 of the individual, particle loading, and other factors (Phalen and Méndez 2009).

338 Although particles are often referred to as insoluble or soluble, it is more appropriate to refer to their
339 dissolution rate in lung fluids, both on RT surfaces and within cells (Phalen et al. 2010). When the
340 dissolution rate is slow compared to the mucus flow or other transport rate, the particles are considered to
341 be *slowly dissolving* or *poorly soluble*. When particles dissolve rapidly, they are considered to be *rapidly*
342 *dissolving*. For simplicity, soluble and insoluble are used herein.

343 Insoluble particles deposited in the ET are typically cleared by bulk physical processes, such as sneezing,
344 coughing, expectoration, or by mucociliary transport followed by swallowing. The latter mechanism is
345 more important for particles deposited in the posterior portions of the nasal region, with the former

346 mechanisms being more important in the anterior nasal region. UF particles also may clear from the ET
347 via the olfactory nerves with direct transport to the brain (to be described later). Both insoluble and
348 soluble particles deposited in the mouth are removed by swallowing or expectoration.

349 Clearance in the TB region of insoluble particles is primarily by mucociliary movement toward the
350 epiglottis where particles are swallowed (ICRP 1994; EPA 2009a). Mucus movement is faster in larger TB
351 airways than in the smaller ones (EPA 2009a; ICRP 1994). This leads to longer residence times for
352 particles deposited deeper in the TB region. Previously, it was assumed that insoluble particles deposited
353 in the TB region were completely cleared by mucociliary action within 24 hr. Recently, this assumption
354 has been shown to be inaccurate, as a fraction of the deposited particles may be retained for much longer
355 time periods (ICRP 1994; Kreyling et al. 2006a, 2006b; Smith et al. 2008; EPA 2009a; Phalen et al.
356 2010). The mechanisms for such slow bronchial clearance include: mucus stasis, mucus retrograde flow,
357 macrophage/epithelial cell uptake, and particle displacement into the subphase of the mucus (EPA 1996,
358 2004, 2009a; Gehr et al. 1990; Schürch et al. 1990). Results summarized in EPA (2009a and references
359 within), indicate that particle clearance from the TB region also is particle size dependent (therefore,
360 deposition location dependent) with probable slower clearance of UF particles (up to several months for
361 complete clearance) and more rapid clearance of particles in the 6-10 μm diameter range. Bolus
362 inhalation studies used to support slow bronchial clearance in humans have been challenged, since it
363 may have been assumed that particles deposited in AI region were actually deposited in the TB airways
364 (Phalen et al. 2010) and the AI region has slower particle clearance than TB region. This assumption
365 would overestimate the fraction of particles that are cleared slowly. Therefore, TB clearance rates are
366 probably more variable, and uncertain than is usually assumed.

367 The primary mechanisms for insoluble particle clearance from the AI region are believed to include: (1)
368 macrophage phagocytosis with subsequent migration to interstitial spaces, i.e., the lymphatics or terminal
369 bronchioles, where the engulfed particles are cleared by mucociliary action; (2) transport in alveolar
370 surface fluids to ciliated airway; or (3) uptake by non-mobile alveolar cells. Macrophage uptake is more
371 efficient for particles larger than 1 μm (Oberdörster 1988), allowing insoluble UF particles to have longer
372 residence times in the AI region, and thus, more time to be taken up by epithelial cells and/or translocate
373 intact across the alveolar epithelium. Translocation, discussed below, is a forth mechanism for particle
374 clearance from the AI region, and noted separately here since the particles remain intact the body.

375 Respiratory tract disease (e.g., acute respiratory infections or COPD) can slow the clearance of insoluble
376 particles from the TB region of the lungs, although there is conflicting information in the literature on this
377 issue as summarized in EPA (2009a), Phalen et al. (2010), Scheuch et al. (2008) and Brown et al. (2002).
378 No difference related to disease was observed in the AI region (EPA 2009a) possibly because RT
379 disease influences where particles deposit, and when there are narrowed RT airways (AI region),
380 particles tend to have more proximal deposition in the lungs. Also, RT infections can slow TB clearance
381 rates, and hence stimulate life-saving coughing fits.

382 Soluble particles dissolve in the lung fluid into their constituents that are cleared by mechanisms that
383 depend on the site of deposition, particle surface area, chemical composition of the particle, particle
384 surface coatings, and molecular weights of the dissolved constituents (EPA 2009a). Soluble particles and
385 constituents may be absorbed by, or diffuse through, the epithelial layers of the TB and AI regions. The
386 rate of this mechanism would be inversely proportional to molecular weight. In the TB region, Lay et al.
387 (2003) observed that mucociliary transport may be slower for soluble than insoluble particles. Water
388 soluble metals may transport through the lung via transepithelial absorption more rapidly than low water
389 or low acid soluble metals and may lead to translocation to other organs within 24 hours (Wallenborn et
390 al. 2007). This is likely important for redox active metals (e.g., often Ni and V as well as Zn, Al, Cd, Fe(II),
391 Pb) (Chen and Lippmann 2009), since they can generate reactive oxygen species (ROS), which can lead
392 to adverse health outcomes.

393 Particle translocation

394 The process of extrapulmonary translocation primarily refers to the migration of particles across the lung
395 fluid and tissue lining to the circulatory systems (Kreyling et al. 2002; Geiser et al. 2005). The
396 mechanisms of translocation are varied including blood and lymph systems, and particle movement
397 through membranes. Once in the circulatory system, particles can translocate to other organs in the body
398 with the potential to cause adverse health effects in the impacted organs (Ferin et al. 1992; Geiser et al.
399 2005; Semmler et al. 2004; EPA 2009a; Nemmar et al. 2002; Mühlfeld et al. 2007; Brown et al. 2002;
400 Oberdörster et al. 2004; Renwick et al. 2004). Under normal physiological conditions, the translocation
401 rate of insoluble particles with diameters larger than about 200 nm is assumed to be negligible (Geiser
402 and Kreyling 2010). After deposition in the AI region, UF particles, which have a longer residence time in
403 the AI region than larger particles, can enter circulation through the air-blood tissue barrier in the alveoli
404 (Geiser et al. 2005). Results indicate that small but detectable amounts of circulating UF particles can
405 accumulate in secondary target organs such as the liver, spleen, heart, kidney, and brain (Kreyling et al.
406 2002; Semmler et al. 2004). The most studied UF particle types included particles composed of carbon,
407 TiO₂, Au, and Ir. For human lungs, however, only one study exists that describes a rapid and significant
408 translocation of inhaled and deposited carbonaceous UF particles to systemic circulation and, thus, to
409 secondary organs (Nemmar et al. 2002). In most other studies translocation for iridium (Kreyling et al.
410 2002) or carbonaceous UF particles was minimal (Mills et al. 2006, Wiebert et al. 2006). It is accepted
411 nowadays that the degree to which inhaled UF particles translocate into the circulatory system is rather
412 small but it is significant (Mühlfeld et al. 2007; Figure 5). However, information on cumulative effects of
413 this translocation process is lacking.

414 Another pathway of UF particle translocation, that does not involve systemic circulation, is transport via
415 the olfactory nerve in the nose to the brain (EPA 2009a; Oberdörster 2010; Phalen et al. 2010 and
416 references within). This latter mechanism was reported in 1934 (Brodie and Elvidge 1934) and recently
417 brought to attention by Oberdörster et al. (2004), and Elder et al. (2006). Translocation of UF particles to

418 the brain from the nose has been observed in several species including humans (EPA 2009a;
419 Oberdörster 2010; Phalen et al. 2010 and references within) and likely occurs in less than an hour.
420 Comparison between rodents and humans may be difficult since rats and mice have much larger olfactory
421 regions of epithelial mucosa (about 50% of the nasal epithelium) than people (about 5%), since humans
422 are more visual than olfactory (Aschner et al. 2005). However the potential health impact of this
423 mechanism is still not understood for air-pollutant particles (Doty 2008, 2009; EPA 2009a; Phalen et al.
424 2010; Oberdörster 2010).

425 *Subject characteristics*

426 Human characteristics that influence particle dose include body size, gender, race, age, and RT disease
427 (the later noted above). Phalen et al. (2010) and EPA (2009a) summarized the effects these parameters
428 have on RT deposition of particles. Dosimetric calculations are often normalized to body weight (or body
429 mass) since airway size, lung volume, and minute ventilation vary with body size. Deposition in average
430 men and average women vary, in part because average women have smaller ET and TB airways, which
431 can shift deposition proximally. This effect can cause greater total deposition in the ET and TB regions;
432 more rapid clearance; and reduced deposition in the AI region. Biological variables, primarily in the ET
433 region influence deposition across race (Phalen et al. 2010, EPA 2009a). In healthy adults, age per-se
434 does not seem to alter deposition; although differences may occur between young children and adults
435 due to body size differences and differences in RT anatomy and ventilation parameters (Bennett and
436 Zeman 2004; Ginsberg et al. 2005; Foos et al. 2008; EPA 2009a).

437 Young children are generally assumed to represent a susceptible population in comparison to adults
438 (O'Neil et al. 2011, this issue). Evidence is limited, but potential effects in children also may include
439 adverse birth outcomes, infant mortality, respiratory effects, such as cough, bronchitis, and asthma
440 attacks, and possibly incomplete lung development. However, such effects are not yet firmly established.

441 Multiple factors affecting particle deposition in children include breathing pattern (healthy young children
442 presumably breathe more through the nose than the mouth), possibly lower efficiency of particle
443 deposition in the nose for children, smaller V_T , faster breathing rate, and differences in airway dimensions
444 and shapes. Modeled and experimental deposition data for children were reviewed and compared by
445 Isaacs and Martonen (2005). Results indicated that the deposited dose per unit surface area of the RT is
446 greater in small children than adults at given similar levels of exertion. Bennett and Zeman (1998)
447 performed clinical studies that indicated that the deposition rate of fine particles normalized to lung
448 surface area might be greater in children than adults. They also noted a correlation of an increased
449 deposition rate in children with higher body mass index, with heavier children having higher V_T and minute
450 ventilation, both which led to a higher deposition rate.

451 Interspecies differences in the clearance of insoluble particles from the TB and AI regions have been
452 noted (Snipes, et al. 1989; Phalen and Méndez 2009; EPA 2009a and references within). Mice and rats,

453 commonly used laboratory subjects, have faster clearance of insoluble particles than people. In the AI
454 and TB region this may be due to shorter distances for removal (e.g., from the AI region, as particles
455 captured by macrophages are transported to the TB region). Also, the lack of respiratory bronchioles in
456 rodents, results in easier access to TB mucus, and thus, may lead to faster clearance.

457 **The Fate of Deposited Particles in the Lung**

458 After having described the fraction which enters into the RT and the mechanisms for deposition and
459 clearance within the RT, the fate of the deposited particles and their effects at the microscopic scale are
460 presented. Specifically, the interactions of UF particles with the internal surface of the airways and the
461 subsequent interaction with cells and cellular sub-structures are described.

462 The focus on UF particles is because research indicates that respiratory and cardiovascular diseases
463 related to inhaled UF particles are frequent and increasing (Schultz *et al.* 2005). UF particles that enter
464 cells are of particular risk because they can cause oxidative stress through the generation of ROS
465 (MacNee 2001). Oxidative stress can cause a reduction in cell metabolic competence via a reduction in
466 mitochondrial respiration as well as an increase in pro-inflammatory cytokine production and other cellular
467 inflammatory reactions and toxicity that can lead to apoptosis, pulmonary and cardiovascular disease, or
468 cancer (Donaldson *et al.* 2003, 2006; Poland *et al.* 2008). The generation of oxidants is likely due to the
469 high organic content and pro-oxidative potential of UF particles (Oberdörster *et al.* 2005). UF particles
470 deposited in the AI region have longer residence times, and thus, more time to interact with cells or
471 translocate through lung tissue and into capillary blood vessels as noted earlier. Epidemiological studies
472 also have convincingly shown the association between UF particles and adverse health effects (Pope *et*
473 *al.* 1995; Peters *et al.* 1997, 2001; Wichmann *et al.* 2000; Künzli *et al.* 2005).

474 Understanding particle interactions at the tissue and cellular level allows for the development of
475 hypotheses regarding possible adverse health effects, appropriate particle metrics, and causal
476 relationships. An important goal of the microscale research is to define the properties of air pollutants
477 and mechanisms of interaction that produce adverse health effects.

478 Particle interactions with pulmonary fluids

479 The fate of inhaled and deposited particles depends on their physicochemical characteristics, deposition
480 location, on the exposed cell types, and on other properties of their microenvironment. Upon deposition,
481 particles contact the internal surface of the RT which is assumed to consist of a continuous extracellular
482 fluid lining from the larynx to the most distal alveoli, including the surfactant (Gehr *et al.* 1990, Schürch *et*
483 *al.* 1990). In the ET and TB airways the fluid layer is thought to consist of two phases, a *sol* phase, in
484 which the cilia beat, and a viscous *gel* phase, the mucus layer (Kilburn 1968). Particle removal is by
485 mechanisms discussed earlier. Throughout the RT, the surfactant system represents a first line of
486 defense (Gehr *et al.* 1996). The composition and structure of the surfactant is complex and varies

487 between airways and alveoli as well as in the AI region during the breathing cycle. In general, it consists
488 of a continuous phospholipid layer containing four different surfactant proteins (Gehr et al. 1990, Schürch
489 et al. 1990) that reduce the surface tension at the air-lung tissue interface to help maintain a particle free
490 surface. This is important in the AI region for gas exchange.

491 Inhaled particles deposited in the RT are displaced into the aqueous subphase below the surfactant film,
492 by surface tensions and possibly other forces exerted on them by the surfactant film (Gehr et al. 1990,
493 Schürch et al. 1990). Particles may be modified by surfactant components or coated with surfactant or
494 surfactant components during the displacement process (Gil and Weiber 1971; Gehr et al. 1990, 1996;
495 Schürch et al. 1990). As a result of the displacement, particles come first into contact with surfactant
496 components in the aqueous subphase and then with the RT epithelium where they may interact with
497 pulmonary cells, such as alveolar or airway epithelial cells and cells of the immune system (e.g.,
498 macrophages and dendritic cells) and be effectively removed from causing potential harm (Geiser et al.
499 2005; Holt and Stumbles 2000; Peters et al. 2004; Vermaelen and Pauwels 2005). In the AI region, UF
500 particles may also translocate into the capillary blood and be transported to elsewhere in the body, as
501 noted earlier. If particles are not removed by these processes, then they can cause pulmonary
502 inflammation by the interaction with cells leading to a range of adverse health effects (de Haar et al.
503 2006).

504 Particle-cell interactions

505 After displacement into the hypophase, inhaled and deposited particles come into close contact with cell
506 membranes, such as those associated with epithelial cells and cells that are part of the immune system
507 and can enter these cells by a range of processes (Brandenberger et al. 2010).

508 All mammalian cells have a common membrane structure that allows or limits what can enter a cell, under
509 most conditions. Cell membranes consist of a very thin film of lipid and numerous protein molecules,
510 mainly held in place by noncovalent interactions (Singer and Nicolson 1972; Kendall 2007). The lipid
511 molecules are arranged as a continuous double layer about 5 nm thick in cell membranes. This lipid
512 bilayer serves as a relatively impermeable barrier to the passage of most water-soluble molecules. The
513 protein molecules are interspersed within, and pass through the lipid bilayer and are referred to as
514 transmembrane proteins. These proteins mediate specific functions, such as transporting molecules
515 across the bilayer or catalyzing membrane-associated reactions. Some proteins serve as structural links
516 that connect the cytoskeleton through the lipid bilayer to the extracellular matrix or an adjacent cell by
517 integrins and cadherins, while others serve as receptors to detect and transduce chemical signals into the
518 cells' environment (Eisenberg et al. 1984).

519 Small molecules can traverse the cellular plasma membrane through the action of protein pumps or
520 channels, while macromolecules must be carried into cells in membrane-bound vesicles derived from the
521 invagination and pinching-off of pieces of the plasma membrane to form endocytic vesicles. Micron-sized

522 particles, which cannot directly penetrate the cellular plasma membrane, enter cells via phagocytosis
523 largely mediated by macrophages, granulocytes and dendritic cells. UF particles can enter the cells via a
524 variety of endocytic pathways or by another, yet to be defined mechanism (Rothen-Rutishauser et al.
525 2007a). Apart from these mechanisms, it has been proposed that UF particles can passively pass
526 through the cellular membrane with subsequent access to subcellular organelles such as the
527 mitochondria and the nucleus (Gehr et al. 2010).

528 Depending on the entry mechanism, particles may be found in vesicles or free in the cellular cytoplasm
529 (Rothen-Rutishauser et al. 2007b; Geiser et al. 2005) (Figure 6). While micron-sized particles are usually
530 found in membrane-bound vesicles, in-vitro studies have shown membrane-free UF particles present in
531 the cytoplasm where they can have direct access to cytoplasmic proteins, and important biochemical
532 molecules in organelles (e.g., the respiratory chain in the mitochondria and the DNA in the nucleus),
533 which may greatly enhance their toxic potential.

534 Once inside the cells, particles transported via endocytic pathways are thought to be distributed non-
535 randomly due to intracellular trafficking pathways. However this might not be the case for UF particles,
536 which can be found free in the cytoplasm. The intracellular trafficking and distribution of particles within
537 the cell is of great interest since it can help identify the relationship among cellular responses and specific
538 intracellular targets. Intracellular trafficking as well as the intracellular location of the particles will have an
539 influence on their effects. However, many knowledge gaps remain in this area due to the technical
540 difficulties of quantifying the intracellular distribution of UF particles, their allocation to specific subcellular
541 structures, and their trafficking.

542 **Dosimetry Modeling of Inhaled Particles**

543 Deposition in the RT is often estimated mathematically based on: (1) semi-empirical models; (2)
544 traditional mechanistic models; or (3) newer sophisticated CFD modeling (Rostami 2009). Studies
545 consider the total (entire RT) and/or regional (ET, TB, AI) deposition, or even more specific subsections
546 within regions. The Association for Inhalation Toxicologists (Alexander et al. 2008) reviewed a number of
547 studies and determined that the total inhaled delivered dose (DD, mg/Kg) can be estimated as follows:

$$548 \quad DD = (C \times RMV \times D \times \eta_i) / BW \quad (\text{Eq. 2})$$

549 Where C is the pollutant concentration in air (mg/L); RVM is respiratory minute volume (L/min); D is the
550 exposure duration (min); η_i is the inhalable fraction; and BW is body weight (kg). This is the dose to
551 which the RT is *exposed*, but not the *deposited* dose. Including a RT deposition term, the deposition
552 fraction, allows for an estimate of the initial total dose delivered and deposited (Alexander et al. 2008;
553 Ginsberg et al. 2005; Méndez et al. 2010). Finlay and Martin (2008) estimated total and regional
554 deposition fractions empirically, based on a review of a number of studies. They proposed separate
555 equations for impaction, sedimentation, and diffusion deposition mechanisms. Separate equations were

556 given for total RT deposition during mouth breathing and nasal breathing, and regional deposition
557 efficiencies.

558 Equation 2 and several semi-empirical models partially based on laboratory data, typically fit the existing
559 clinical data well, but have limited predictive value for situations that were not tested. More complex
560 traditional mechanistic mathematical models apply simplifying assumptions regarding airway structure to
561 predict deposition in major regions of the RT based on particle deposition mechanisms (e.g. ICRP 1994,
562 1995). Traditional models include the ICRP (International Commission on Radiation Protection) and the
563 multiple path particle dosimetry (MPPD, http://www.ara.com/products/mppd_capabilities.htm) models.
564 These models have been used to compare inhalation deposition in rats and humans Brown et al. (2005)
565 and for adults versus children (3-mo old) by RT region Ginsberg et al. (2005). A comparison of these
566 models is given in Figure 2 for both nose and mouth breathing, for rest (Figure 2a) and light exercise
567 (Figure 2b), and for total and major RT regions (ET, TB, and AI) (EPA (2009a; ICRP 1995).

568 CFD models are even more sophisticated, being based on fundamental equations of airflow structure
569 using iterative numerical techniques (Rostami 2009). In CFD models, particles are introduced into the
570 predicated flow fields and deposit where they cross an airway-wall boundary. Many assumptions are
571 used in CFD modeling, such as isothermal airflow, rigid airways, and spherical non-interacting particles.
572 Challenges in validating CFD models are discussed in Oldham (2006). More recently, lung structure is
573 being obtained by medical imaging techniques, such as magnetic resonance imaging, positron emission
574 tomography, computed tomography, and ultrasound. Digitized data obtained from these methods
575 potentially allow for more detailed and reliable CFD simulations of particle deposition using more realistic
576 lung morphology. Results are dependent on numerous selectable inputs that still require validation. Also,
577 due to the complexity of the pulmonary region, CFD models currently model only limited airway regions,
578 e.g., from the nose and mouth to the 15th airway generation (Kleinstreuer and Zhang 2010). An example
579 of CFD modeling is given in Figure 4 for UF (NP) particles and micrometer sized particles. From this
580 figure, it is easy to see hot spots that develop for both UF particles and micrometer sized particles as well
581 as the more uniform deposition for UF particles throughout the upper RT, as noted earlier.

582 **Areas of Future Research**

583 Significant advancements have occurred over the last 5-7 years with regards to particle dosimetry as
584 touched upon in this paper. However, as understanding has improved, many new questions have arisen
585 that once addressed should further reduce uncertainty in estimating particle dose that will provide
586 important information for health researchers examining mechanisms and the adverse health effects of PM
587 pollution. Listed here is a subset of suggested research that should further reduce uncertainties across
588 the source-to-dose-to-health effects continuum.

589 *Source to Intake:*

- 590
- 591
- 592
- 593
- 594
- 595
- 596
- 597
- 598
- 599
- 600
- 601
- 602
- 603
- *iF* values should be obtained for scenarios in more developing countries, where urban population densities greatly exceed those in the developed world, where there are significantly more people on the streets receiving high levels of exposure, and where buildings likely allow for greater infiltration of particles.
 - Further work should be done differentiating the *iF* resulting from exposures to low socio-economic status individuals and those of higher socio-economic status, as those with lower socio-economic status may be more vulnerable to exposures to PM as a result of living and working close to pollution sources.
 - Continued communication with policy makers is needed to determine how to provide *iF* values with the needed attributes to best incorporate this tool into policy decisions, enabling them to determine the most efficient way for reducing PM exposures to improve health.
 - Chemical processes in the atmosphere, including the formation of secondary pollutants and movement of pollutants between the gas and solid/liquid phases should be more clearly elucidated for incorporation into *iF* calculations.

604 *Fate in the Respiratory Tract*

- 605
- 606
- 607
- 608
- 609
- 610
- 611
- 612
- 613
- 614
- 615
- 616
- 617
- 618
- 619
- 620
- 621
- 622
- 623
- 624
- Identification of the appropriate dose metrics for PM, given the great variability of particles, exposed populations, and potential health effects, represents a major important challenge. Specifically, each adverse health-effect scenario may require an evaluation of the proper metric, or metrics.
 - Understanding differences in the delivered dose among species, within strains, and animal models that are created by pretreatment to produce diseases will improve our understanding of the impact of these diseases in humans.
 - Quantifying differences in deposition patterns, clearance phenomena, and air-pollutant effects in human subpopulations due to differences in anatomy and physiology, (e.g., for children, the elderly and the diseased) is needed to reduce uncertainty in dosimetric calculations, and the impact of changes in lung morphology due to differences among humans.
 - Translating results between animal studies to *in-vitro* studies and from animal studies and from *in-vitro* studies to humans, particularly as far as dose is concerned is critical since many needed studies cannot be directly performed using human subjects, due to practical and ethical constraints.
 - Computational fluid dynamic (CFD) models of PM deposition hold great promise for calculating local and regional deposition doses. Improvements are needed in computational capabilities to allow for a greater extent of the lung to be modeled and models should be more thoroughly evaluated, In additional, advances in medical imaging approaches should allow for more detailed airway morphometric data assisting computational studies to model beyond the 16th TB branch.

- 625 • Most traditional mechanistic and CFD dosimetric models are validated for ideal particles (e.g.
626 smooth, uncharged, spheres). Realistic environmental particles are, as yet, to be modeled leaving
627 significant uncertainty with regards to actual dose for ambient PM..
- 628 • Measuring and modeling particle deposition hot spots, quantifying enhancement factors
629 associated with hot spots, and verifying modeling results are needed to understand the
630 toxicological significance of hot spots.
- 631 • The influence of particle size and other properties on the mechanisms driving slow-bronchial
632 clearance still need to be elaborated since this process may drive the fraction of particles and
633 components retained in the lungs and allows UF particles to translocate across the air-blood
634 tissue barrier to other parts of the body .

635 *Tissue, Cellular, and Sub-cellular Interactions*

- 636 • UF particles, their translocation, micro dosimetry, and health effects, are still in an early phase of
637 understanding, although significant progress has occurred over the last decade. Engineered NPs
638 represent a vast area of research that is just beginning to be explored as these particles become
639 widely used in commercial applications.
- 640 • A major research frontier involves elucidating the interactions of PM, in its great variability, with
641 the varied cells of the body. The complexities of particle fates in cells and the resulting potential
642 toxicities (e.g. cytotoxicity, genotoxicity, immunotoxicity) and cascades of biological responses
643 are still at the beginning of being understood.
- 644 • The coating of airborne particles (outside the body) with potentially toxic substances and the
645 coating of the particles upon interaction with body fluids, tissues, and cells is just beginning to be
646 investigated and is poorly understood. Coating with fluids of any kind, i.e., coating most likely with
647 proteins, may be the key to better understand toxicity and health effects.
- 648 • The mechanism of entry into cells and specifically, interactions of UF particles with subcellular
649 structures and possible enhancements in particle toxicity due to these interactions is recent area
650 of research that should be pursued to better understand the mechanisms that drive PM health
651 effects.

652 **Summary**

653 This paper provides a brief summary of the current science associated with air pollution dosimetry and
654 begins to address the forth policy-relevant Science Question addressed in part at 2010 International Air
655 Pollution and Health conference². The paper begins at the macroscale describing the definition and

² Air Pollution and Health, 2010 (Solomon et al. 2011) SQ4: “What advances have been made in understanding the relationships between exposure, both spatially and temporally, and estimates of dose that tie to health outcomes?”

656 attributes of the intake fraction (iF), a parameter that provides an estimate of the amount of pollutant
657 inhaled (not deposited or retained) relative to the mass emitted into the environment and allows for a
658 better understanding and quantification of source-to-intake (inhaled) relationships. Inhalation of air
659 pollution is the first step in dosimetry since the respiratory tract (RT) is the primary route for air pollutants
660 to enter the body. The dimensionless parameter, iF , also allows for evaluation of how the amount inhaled
661 of a pollutant might vary as a function of emissions control strategies or other interventions (van Erp et al.
662 2011, this issue) that reduce pollutant concentrations from a source(s). The next section describes what
663 happens once a pollutant is inhaled and provides updates on recent advances in dosimetry and factors
664 that relate to quantifying dose. A description of the processes and mechanisms of how pollutants,
665 specifically particles, are deposited and cleared from the RT is given. Translocation, the movement of
666 particles from the lungs to other parts of the body, also is discussed.

667 Looking at the microscale, the next section examines how UF particles interact at the cellular and sub-
668 cellular levels. UF particles constitute a unique size range that recently has been identified as a key
669 pollutant of interest, since they can penetrate deep into the lungs and have the ability to cross the air-
670 blood barrier of the lung and translocate to other systems and organs. UF particles also have been
671 shown to translocate to the brain directly from inside the nose.

672 Considerable uncertainty remains with regards to UF particle interactions within the RT, in part because
673 most of the experimental data, except for the epidemiological data, have been obtained from animal and
674 in vitro experiments. Data received from these experiments are providing a significant basic idea of how
675 adverse health effects develop, but the extrapolation to humans is still not well defined and additional
676 research is needed to better understand the adverse health effects of ultrafine particles in people.

677 The last section describes dosimetric modeling from semi-empirical to CFD modeling. Continued
678 advances in application of medical imaging techniques to provide digital data bases for CFD models will
679 allow CFD models to simulate the lower TB and AI regions of the lung.

680 A series of research needs also is presented

681 **Acknowledgements**

682 The preparation of this informative summary, in response to the forth policy-relevant Science Question
683 that was addressed in part at the 2010 International Air Pollution and Health conference², was supported
684 in part by the Charles S. Stocking Family Trust (Dr. Phalen) and the CA Air Resources Board ARB-08-
685 306 (Dr. Méndez). The group from Switzerland received generous financial support from the Swiss
686 National Science Foundation, the Deutsche Forschungsgemeinschaft, the Animal Free Research
687 Foundation, the Gottfried and Julia Bangerter-Rhyner-Foundation, the Doerenkamp-Zbinden Foundation,
688 the Foundation Johanna-Dürmüller-Bol, the Lungenliga Schweiz and the Swiss Federal Office for the
689 Environment is greatly appreciated. The authors declare that they have no conflict of interest and do not

690 have a financial relationship with the sponsors of the conference. The U.S. Environmental Protection
691 Agency through its Office of Research and Development partially funded and managed the development
692 of this journal article. It has been subjected to the Agency's administrative review and approved for
693 publication. Mention of trade names or commercial products does not constitute endorsement or
694 recommendation for use.

695

696 **References**

697 Alexander DJ, Collins CJ, Coombs DW, Gilkison IS, Hardy CJ, Healey G, Karantabias G, Johnson N,
698 Karlsson A, Kilgour JD, McDonald P (2008) Association of Inhalation Toxicologists (AIT) Working Party
699 recommendation for standard delivered dose calculation and expression in nonclinical aerosol inhalation
700 toxicology studies with pharmaceuticals. *Inhal Toxicol* 20:1179–1189.

701 Aschner M, Erikson KM, Dorman DC (2005) Manganese dosimetry: Species differences and implications
702 for neurotoxicity. *Crit Rev Toxicol* 35:1-32.

703 Balásházy I, Hofmann W, Heistracher T (1999) Computation of local enhancement factors for the
704 quantification of particles deposition patterns in airway bifurcations. *J Aerosol Sci* 30:185-203.

705 Balásházy I, Hofmann W, Heistracher T (2003) Local particle deposition patterns may play a key role in
706 the development of lung cancer. *J Appl Physiol* 94:1719-1725.

707 Bennett WD, Zeman KL (1998) Deposition of fine particles in children spontaneously breathing at rest.
708 *Inhal Toxicol* 10:831-842.

709 Bennett WD, Zeman KL (2004) Effect of body size on breathing pattern and fine-particle deposition in
710 children. *J Appl Physiol* 97:821-826.

711 Bennett WD, Zeman KL, Kim C, Mascarella J (1997) Enhanced deposition of fine particles in COPD
712 patients spontaneously breathing at rest. *Inhal Toxicol* 9:1-14.

713 Bennett, D.H., Mckone T, Evans, J, Nazaroff W, Margni M, Jolliet O, Smith K (2002a) Defining intake
714 fraction. *Environ Sci Technol* 36(9):207A-211A.

715 Bennett DH, Margni M, McKone TE, Jolliet O (2002b) Intake fraction for multimedia pollutants: A tool for
716 life cycle analysis and comparative risk assessment. *Risk Analysis* 22(5):905-918.

717 Brandenberger C, Mühlfeld C, Zulqurnain A, Lenz AG, Schmit O, Parak WJ, Gehr P, Rothen-Rutishauser
718 B (2010) Quantitative Evaluation of Cellular Uptake and Trafficking of Plain and Polyethylene Glycol-
719 Coated Gold Nanoparticles. *Small* 6:1669-1678.

720 Brodie M, Elvidge AR (1934) The portal of entry and transmissions of the virus of poliomyelitis. *Science*
721 79(2045):235-236.

722 Brook RD, Rajagopalan S, Pope CA III, Brook JR, Bhatnagar A, Diez-Roux AV, Holguin F, Hong Y,
723 Luepker RV, Mittleman MA, Peters A, Siscovick D, Smith SC Jr, Whitsel L, Kaufman JD, on behalf of the
724 American Heart Association Council on Epidemiology and Prevention, Council on the Kidney in
725 Cardiovascular Disease, and Council on Nutrition, Physical Activity and Metabolism (2010) Particulate
726 matter air pollution and cardiovascular disease: an update to the scientific statement from the American
727 Heart Association. *Circulation* 121:2331–2378.

728 Brown JS, Zeman KL, Bennett WD (2002) Ultrafine particle deposition and clearance in the healthy and
729 obstructed lung. *Am J Respir Crit Care Med* 166:1240-1247.

730 Brown JS, Wilson WE, Grant LD (2005) Dosimetric comparisons of particle deposition and retention in
731 rats and humans. *Inhal Toxicol* 17:355–385.

732 Chang L-Y, Crapo JD, Gehr P, Rothen-Rutishauser B, Mühlfeld C, Blank F (2010) Alveolar epithelium in
733 lung toxicology. In: *Comprehensive Toxicology*, Vol 8, Respiratory Toxicology, ed. Yost GS. Elsevier,
734 Amsterdam, pp. 59-91.

735 Chen LC, Lippmann M (2009) Effects of metals within ambient air particulate matter (PM) on human
736 health. *Inhal Toxicol* 21:1-31.

737 De Haar C, Hassing I, Bol M, Bleumink R, Pieters R (2006) Ultrafine but not fine particulate matter causes
738 airway inflammation and allergic airway sensitization to co-administered antigen in mice. *Clin Exp Allergy*
739 36:1469-1479.

740 Donaldson K, Stone V, Borm PJ, Jimenez LA, Gilmour PS, Schins RPF, Knaapen AM, Rahman I, Faux
741 SP, Brown DM, MacNee W (2003) Oxidative stress and calcium signaling in the adverse effects of
742 environmental particles (PM₁₀). *Free Radic Biol Med* 34:1369-1382.

743 Donaldson K, Aitken R, Tran L, Stone V, Duffin R, Forrest G, Alexander A (2006) Carbon nanotubes: A
744 review of their properties in relation to pulmonary toxicology and workplace safety. *Toxicol Sci* 92:5-22.

745 Doty RL (2008) The olfactory vector hypothesis of neurodegenerative disease: Is it viable? *Annals Neurol*
746 63:7-15.

747 Doty RL (2009) Do environmental agents enter the brain via the olfactory mucosa to induce
748 neurodegenerative diseases? *NY Acad Sci* 1170:610-614.

749 Eisenberg D, Schwarz E, Komaromy M, Wall R (1984) Analysis of membrane and surface protein
750 sequences with the hydrophobic moment plot. *J Mol Biol* 179:125-142.

751 Elder A, Gelein R, Silva V, Feikert T, Opanashuk L, Carter J, Potter R, Maynard A, Ito Y, Finkelstein J,
752 Oberdörster G (2006) Translocation of inhaled ultrafine manganese oxide particles to the central nervous
753 system. *Environ Health Perspect* 114:1172-1178.

754 EPA (1996) Air quality criteria for particulate matter. U.S. Environmental Protection Agency, National
755 Center for Environmental Assessment. Research Triangle Park, NC, EPA/600/P-95/001aF-cF.
756 <http://www.epa.gov/nheerl/research/pm/references.html> (accessed 8-23-11)

757 EEPA (2004) Air quality criteria for particulate matter (Final Report, Oct 2004). U.S. Environmental
758 Protection Agency, Washington, DC, EPA/600/P-99/002aF-bF.
759 http://cfpub.epa.gov/si/si_public_record_report.cfm?dirEntryId=87903 (Accessed 8-23-11)

760 EPA (2009a) Integrated science assessment for particulate matter (Final Report). U.S. Environmental
761 Protection Agency, National Center for Environmental Assessment. Washington, DC, EPA/600/R-
762 08/139F. <http://cfpub.epa.gov/ncea/isa/recordisplay.cfm?deid=216546> (Accessed 8-23-11)

763 Farkas A, Balásházy I (2008) Quantification of particle deposition in asymmetrical tracheobronchial model
764 geometry. *Comput Biol Med* 38:508-518.

765 Ferin J, Oberdörster G, Penney DP (1992) Pulmonary retention of ultrafine and fine particles in rats. *Am J*
766 *Respir Cell Mol Biol* 6:535-542.

767 Finlay WH, Martin AR (2008) Recent advances in predictive understanding of respiratory tract deposition.
768 *J Aerosol Med Pulm Drug Deliv* 21:189–206.

769 Finlayson-Pitts BJ, Pitts JN Jr (2000) *Chemistry of the Upper and Lower Atmosphere, Theory,*
770 *Experiments, and Applications.* Academic Press. San Diego, CA, 969 pp.

771 Foos B, Marty M, Schwartz J, Bennett W, Moya J, Jarabek AM, Salmon AG (2008) Focusing on children's
772 inhalation dosimetry and health effects for risk assessment: An introduction. *J Toxicol Environ Health A*
773 71:149-165.

774 Gallo, MA (2008) History and scope of toxicology. In Casarett & Doull's *Toxicology: The Basic Science of*
775 *Poisons*, 7th edition, ed Klassen, CD, McGraw Hill, New York, NY, pp. 3-10.

776 Gehr P, Bachofen H, Weibel ER (1978) The normal human lung: ultrastructure and morphometric
777 estimation of diffusion capacity. *Respir Physiol* 32:121-140.

778 Gehr P, Schürch S, Berthiaume Y, Im Hof V, Geiser M (1990) Particle retention in airways by surfactant. *J*
779 *Aerosol Med* 3:27-43.

780 Gehr P, Green FH, Geiser M, Im Hof V, Lee MM, and Schurch S (1996) Airway surfactant, a primary
781 defense barrier: mechanical and immunological aspects. *J Aerosol Med* 9:163-181.

782 Gehr P, Muhfeld C, Rothen-Ruthishhauser B, Blank F, eds. (2010) *Particle-Lung Interactions*, 2nd edn.,
783 Informa Healthcare, New York, NY, 319 pp.

784 Geiser M, Kreyling WG (2010) Deposition and biokinetics of inhaled nanoparticles. *Part Fibre Toxicol* 7:2,
785 doi:10.1186/1743-8977-7-2.

786 Geiser M, Rothen-Rutishauser B, Kapp N, Schürch S, Kreyling W, Schulz H, Semmler M, Im Hof V,
787 Heyder J, Gehr P (2005) Ultrafine particles cross cellular membranes by nonphagocytic mechanisms in
788 lungs and in cultured cells. *Environ Health Perspect* 113:1555-1560.

789 Gerde P (2008) How do we compare dose to cells in vitro with dose to live animals and humans? Some
790 experiences with inhaled substances. *Exp Toxicol Pathol* 60:181–184.

791 Gil J, Weibel ER. (1971) Extracellular lining of bronchioles after perfusion-fixation of rat lungs for electron
792 microscopy. *Anat Rec* 169:185-199.

793 Ginsberg GL, Foos BP, Firestone MP (2005) Review and analysis of inhalation dosimetry methods for
794 application to children's risk assessment. *J Toxicol Environ Health A* 68:573–615.

795 Greco SL, Wilson AM, Hanna SR, Levy JI (2007a) Factors influencing mobile source particulate matter
796 emissions-to-exposure relationships in the Boston urban area. *Environ Sci Technol* 41:7675-7682.

797 Greco SL, Wilson AM, Spengler JD, Levy JI (2007b) Spatial patterns of mobile source particulate matter
798 emissions-to-exposure relationships across the United States. *Atmos Environ* 41:1011-1025.

799 Hao J, Wang L, Shen M, Li L, Hu J (2007) Air quality impacts of power plant emissions in Beijing. *Environ*
800 *Pollut* 147:401-408.

801 He F, Shaffer ML, Li X, Rodriguez-Colon S, Wolbrette DL, Williams R, Cascio WE, Liao D (2011)
802 Individual-level PM_{2.5} exposure and the time course of impaired heart rate variability: The APACR Study.
803 *J Expo Sci Environ Epidemiol* 21:65–73.

804 Heath GA, Granvold PW, Hoats AS, Nazaroff WW (2006) Intake fraction assessment of the air pollutant
805 exposure implications of a shift toward distributed electricity generation. *Atmos Environ* 40:7164-7177.

806 Holt PG, Stumbles PA. (2000) Characterization of dendritic cell populations in the respiratory tract. *J*
807 *Aerosol Med* 13:361-367.

808 Humbert S, Marshall JD, Shaked S, Spadaro JV, Nishioka Y, Preiss P, McKone TE, Horvath A, Jolliet O
809 (2011) Intake fraction for particulate matter: recommendations for life cycle impact assessment. *Environ*
810 *Sci Technol* 45:4808-4816.

811 ICRP (International Commission on Radiological Protection) (1994) Human Respiratory Tract Model for
812 Radiological Protection. ICRP Publication No. 66. Tarrytown, NY: Elsevier Science Ltd..

813 ICRP (1995) Human respiratory tract model for radiological protection: A report of a task group of the
814 International Commission on Radiological Protection. *Ann ICRP* 24, 482 pp.

815 Isaacs KK, Martonen TB (2005) Particle deposition in children's lungs: Theory and experiment. *J Aerosol*
816 *Med* 18:337–353.

817 Kendall M. (2007) Fine airborne urban particles (PM_{2.5}) sequester lung surfactant and amino acids from
818 human lung lavage. *Am J Physiol Lung Cell Mol Physiol* 293:L1053-L1058.

819 Kilburn KH. (1968) A hypothesis for pulmonary clearance and its implications. *Am Rev Respir Dis* 98:449-
820 463.

821 Kleinstreuer C, Zhang Z (2010) Airflow and particle transport in the human respiratory system. *Ann Rev*
822 *Fluid Mech* 42:301-334.

823 Klepeis NE, Nazaroff WW (2006) Modeling residential exposure to secondhand tobacco smoke. *Atmos*
824 *Environ* 40(23):4393-4407.

825 Kreyling WG, Semmler M, Erbe F, Mayer P, Takenaka S, Schulz H, Oberdörster G, Ziesenis A (2002)
826 Translocation of ultrafine insoluble iridium particles from lung epithelium to extrapulmonary organs is size
827 dependent but very low. *J Toxicol Environ Health A* 65:1513-1530.

828 Kreyling WG, Sammler-Behnke M, Möller W (2006a) Health implication of nanoparticles. *J Nanoparticle*
829 *Rsh* 8:543-562.

830 Kreyling WG, Sammler-Behnke M, Möller W (2006b) Ultrafine particle-lung interactions: does size matter?
831 *J Aerosol Med* 19:74-83.

832 Künzli N, Jerrett M, Mach WJ, Beckerman B, LaBree L, Gilliland F, Thomas D, Peters J, Hodis HN (2005)
833 Ambient Air Pollution and Atherosclerosis in Los Angeles. *Environ Health Perspect* 113:201-206.

834 Lay JC, Stang MR, Fisher PE, Yankaskas JR, Bennett WD (2003) Airway retention of materials of
835 different solubility following local intrabronchial deposition in dogs. *J Aerosol Med* 16:153-166.

836 Levy JI, Baxter LK, Schwartz J (2009) Uncertainty and variability in health-related damages from coal-
837 fired power plants in the United States. *Risk Ana* 29:1000-1014.

838 Li, J., J.M. Hao (2003) Application of intake fraction to population exposure estimates in Hunan Province
839 of China. *J Environ Sci Health A Tox Hazard Subst Environ Eng* 38(6):1041-1054.

840 Luo Z, Li Y, Nazaroff WW (2010) Intake fraction of nonreactive motor vehicle exhaust in Hong Kong.
841 *Atmos Environ* 44:1913-1918.

842 MacNee W (2001) Oxidative stress and lung inflammation in airways disease. *Eur J Pharmacol* 429:195-
843 207.

844 Marshall JD, Behrentz E (2005) Vehicle self-pollution intake fraction: Children's exposure to school bus
845 emissions. *Environ Sci Technol* 39:2559-2563.

846 Mauderly et al. 2011, this issue

847 Méndez LB, Gookin G, Phalen RF (2010) Inhaled aerosol particle dosimetry in mice: A review. *Inhal*
848 *Toxicol* 22S2:15–20.

849 Mills NL, Amin N, Robinson SD, Anand A, Davies J, Patel D, de la Fuente JM, Cassee FR, Boon NA,
850 Macnee W, Millar AM, Donaldson K, Newby DE (2006) Do inhaled carbon UF particles translocate directly
851 into the circulation in humans? *Am J Respir Crit Care Med* 173:426-431.

852 Mühlfeld C, Geiser M, Kapp N, Gehr P, Rothen-Rutishauser B (2007) Re-evaluation of pulmonary
853 titanium dioxide nanoparticle distribution using the “relative deposition index”: Evidence for clearance
854 through microvasculature. *Part. Fibre Toxicol.* 4:7, doi:10.1186/1743-8977-4-7.

855 Nemmar A, Hoet PH, Vanquickenborne B, Dinsdale D, Thomeer M, Hoylaerts MF, Vanbilloen H,
856 Mortelmans L, Nemery B (2002) Passage of inhaled particles into the blood circulation in humans.
857 *Circulation* 105:411-414.

858 NRC Research Priorities for Airborne Particulate Matter (1998) I. Immediate Priorities and a Long-Range
859 Research Portfolio. National Research Council, National Academies Press: Washington, DC, 195 pp.

860 O’Neil et al. 2011, this issue.

861 Oberdörster G (1988) Lung clearance of inhaled insoluble and soluble particles. *J Aerosol Med* 1:289-
862 330.

863 Oberdörster G (2010). Safety assessment for nanotechnology and nanomedicine: concepts of
864 nanotoxicology. *J Intern Med* 267:89–105.

865 Oberdörster G, Sharp Z, Atudorei V, Elder A, Gelein R, Kreyling W, Cox C (2004) Translocation of inhaled
866 ultrafine particles to the brain. *Inhal Toxicol* 16:437-445.

867 Oberdörster G, Maynard A, Donaldson K, Castranova V, Fitzpatrick J, Ausman K, Carter J, Karn B,
868 Kreyling W, Lai D, Olin S, Monteiro-Riviere N, Warheit D, Yang H (2005) Principles for characterizing the
869 potential human health effects from exposure to nanomaterials: elements of a screening strategy. *Part*
870 *Fibre Toxicol* 2:8, doi:10.1186/1743-8977-2-8, doi: 10.1186/1743-8977.

871 Oldham MJ (2006) Challenges in validating CFD-derived inhaled aerosol deposition predictions. *Inhal*
872 *Toxicol* 18:781–786.

873 Peters A, Wichmann HE, Tuch T, Heinrich J, Heyder J (1997) Respiratory effects are associated with the
874 number of ultrafine particles. *Am. J Respir Crit Care Med* 155:1376-1383.

875 Peters A, Dockery DW, Muller JE, Mittleman MA (2001) Increased particulate air pollution and the
876 triggering of myocardial infarction. *Circulation* 103:2810-2815.

877 Peters-Golden M (2004) The alveolar macrophage: the forgotten cell in asthma. *Am J Respir Cell Mol Biol*
878 31:3-7.

879 Phalen RF, Méndez LB (2009) Dosimetry considerations for animal inhalation studies. *Biomarkers*
880 14(S1):63–66.

881 Phalen RF, Oldham MJ, Nel AE (2006) Tracheobronchial particle dose considerations for In-vitro
882 toxicology studies. *Toxicol Sci* 92:126-132.

883 Phalen RF, Méndez LB, Oldham MJ (2010) New developments in aerosol dosimetry. *Inhal Toxicol*
884 22(S2):6-14.

885 Poland CA, Duffin R, Kinloch I, Maynard A, Wallace WA, Seaton A, Stone V, Brown S, MacNee W,
886 Donaldson K (2008) Carbon nanotubes introduced into the abdominal cavity of mice show asbestos-like
887 pathogenicity in a pilot study. *Nat Nanotechnol* 3:423-428.

888 Pope CA III, Dockery DW, Schwartz J (1995) Review of epidemiological evidence of health effects of
889 particulate air pollution. *Inhal. Toxicol.* 7:1-18.

890 Pope CA III, Ezzati M, Dockery DW (2009) Fine-particulate air pollution and life expectancy in the United
891 States. *N Engl J Med* 360:376-386.

892 Puett RC, Hart JE, Yanosky JD, Paciorek C, Schwartz J, Suh H, Speizer FE, Laden F (2009) Chronic fine
893 and coarse particulate exposure, mortality, and coronary heart disease in the Nurses' Health Study.
894 *Environ Health Perspect* 117:1697-1701.

895 Renwick LC, Brown D, Clouter A, Donaldson K (2004) Increased inflammation and altered macrophage
896 chemotactic responses caused by two ultrafine particle types. *Occup Environ Med* 61:442-447.

897 Ries FJ, Marshall JD, Brauer M. (2009) IF of urban wood smoke. *Environ Sci Technol* 43:4701-4706.

898 Rostami AA (2009) Computational modeling of aerosol deposition in (the) respiratory tract: A review. *Inhal*
899 *Toxicol* 21:262-290.

900 Rothen-Rutishauser B, Mühlfeld C, Blank F, Musso C, Gehr P (2007a) Translocation of particles and
901 inflammatory responses after exposure to fine particles and nanoparticles in an epithelial airway model.
902 *Part Fibre Toxicol* 4:9, doi:10.1186/1743-8977-4-9

903 Rothen-Rutishauser B, Schürch S, Gehr P (2007b) Interaction of particles with membranes. In: *Particle*
904 *Toxicology*. Donaldson K, Borm P eds.. Taylor & Francis Group, LLC, CRC Press, Boca Raton, FL, pp.
905 139-160.

906 Scheuch G, Kohlhäufel M, Möller W, Brand P, Meyer T, Häussinger K, Sommerer K, Heyder J (2008)
907 Particle clearance from the airways of subjects with bronchial hyperresponsiveness and with chronic
908 obstructive pulmonary disease. *Exp Lung Res* 34:531-549.

909 Schultz H, Harder V, Ibaldo-Mulli A, Khandoga A, Koenig W, Krombach F, Radykewicz R, Stampfl A,
910 Thorand B, Peters A (2005) Cardiovascular effects of fine and ultrafine particles. *J Aerosol Med* 18:1-22.

911 Schürch S, Gehr P, Im Hof V, Geiser M, Green F (1990) Surfactant displaces particles toward the
912 epithelium in airways and alveoli. *Respir Physiol* 80:17-32.

913 Seinfeld JH, Pandis SN (1998) Atmospheric Chemistry and Physics from Air Pollution to Climate Change.
914 New York, NY: John Wiley and Sons, Inc. 1326 pp..

915 Semmler M, Seitz J, Erbe F, Mayer P, Heyder J, Oberdörster G, Kreyling WG (2004) Long-term clearance
916 kinetics of inhaled ultrafine insoluble iridium particles from the rat lung, including transient translocation
917 into secondary organs. *Inhal Toxicol* 16:453-459. Sheppard L, Burnett RT, Szpiro AA, Kim S-Y, Jerrett M,
918 Pope CA III, Brunekreef B (2011) Confounding and exposure measurement error in air pollution
919 epidemiology. *Air Qual Atmos Health* DOI 10.1007/s11869-011-0140-9.

920 Singer SJ, Nicolson GL. (1972) The fluid mosaic model of the structure of cell membranes. *Science*
921 175:720-731.

922 Smaldone GC, Foster WM, O'Riordan TG, Messina MS, Perry RJ, Langenback EG (1993) Regional
923 impairment of mucociliary clearance in chronic obstructive pulmonary disease. *Chest* 103:1390-1396.

924 Smith JRH, Bailey MR, Etherington G, Shutt AC, Youngmann MJ (2008) Effect of particle size on slow
925 particle clearance from the bronchial tree. *Exp Lung Res* 34:287-312.

926 Snipes MB, McClellan RO, Mauderly JL, Wolff RK (1989) Retention patterns for inhaled particles in the
927 lung: comparisons between laboratory animals and humans for chronic exposures. *Health Phys*
928 57(S1):69-78.

929 Solomon PA, Costantini M, Grahame TJ, Gerlofs-Nijland ME, Cassee F, Russell AG, Brook JR, Hopke
930 PK, Hidy G, Phalen RF, Saldiva P, Ebel Sarnat S, Balmes JR, Tager IB, Özkaynak H, Vedal S, Wierman
931 SSG, Costa DL (2011) Air pollution and health: Bridging the gap from sources to health outcomes:
932 conference summary. *Air Qual Atmos Health* accepted for publication, 2011.

933 Stevens G, de Foy B, West JJ, Levy JI (2007) Developing intake fraction estimates with limited data:
934 Comparison of methods in Mexico City. *Atmos Environ* 41:3672-3683.

935 Tainio M, Sofiev M, Hujo M, Tuomisto JT, Loh M, Jantunen MJ, Karppinen A, Kangas L, Karvosenoja N,
936 Kupiainen K, Porvari P, Kukkonen J (2009) Evaluation of the European population intake fractions for
937 European and Finnish anthropogenic primary fine particulate matter emissions. *Atmos Environ* 43:3052-
938 3059.

939 van Erp AM, Kelly FJ, Demerjian KD, Pope CA III, Cohen AJ (2011) Progress in research to assess the
940 effectiveness of air quality interventions towards improving public health. *Air Qual Atmos Health* DOI
941 10.1007/s11869-010-0127-y.

942 Vermaelen K, Pauwels R. (2005) Pulmonary dendritic cells. *Am J Respir Crit Care Med* 172:530-551.

943 Wallenborn JG, McKee JK, Schladweiler MC, Ledbetter AD, Kodavanti UP (2007) Systemic translocation
944 of particulate matter-associated metals following a single intratracheal instillation in rats. *Toxicol Sci*
945 98:231-239.

946 Wang SX, Hao J, Ho MS, Li J, Lu Y (2006) Intake fractions of industrial air pollutants in China: estimation
947 and application. *Sci Total Environ* 354:127-141.

948 Wichmann HE, Spix C, Tuch T, Wolke G, Peters A, Heinrich J, Kreyling WG, Heyder J. (2000) Daily
949 mortality and fine and ultrafine particles in Erfurt, Germany, part I: role of particle number and particle
950 mass. *Res Rep Health Eff Inst* 98:5-94.

951 Wiebert P, Sanchez-Crespo A, Falk R, Philipson K, Lundin A, Larsson S, Möller W, Kreyling WG,
952 Svartengren M (2006) No significant translocation of inhaled 35-nm carbon particles to the circulation in
953 humans. *Inhal Toxicol* 18:741-747.

954 Zhang Z, Kleinstreuer C, Donohue JF, Kim CS (2005). Comparison of micro- and nano-size particle
955 depositions in a human upper airway model. *J Aerosol Sci* 36:211–33.

956 Zhou Y , Levy JI (2008) The impact of urban street canyons on population exposure to traffic-related
957 primary pollutants. *Atmos Environ* 42:3087-3098.

958

Table 1. Some particle-related that may apply to the effects of inhaled air-pollutant particles. Note that these properties are not mutually exclusive.

Mass related to aerodynamic size intervals (e.g. PM₁₀, PM_{2.5}, and coarse particles)

Size distribution properties (e.g. geometric standard deviation)

Number per unit volume of air

Surface area (e.g. BET surface), or projected area

Surface reactivity in the body

Chemical composition (e.g., metals (e.g., V, Ni), acids, OC, EC (or BC), organic species etc.)

Oxidative properties (e.g., reactive oxygen potential)

Mobility within the body

Fractal properties

Electrical properties (e.g. net charge and/or zeta potential)

Dissolution rates in biological fluids and other media

Volatility of particle components

Shape (e.g. aspect ratio of fibers)

Infectivity, irritancy, allergenicity, and odor (odor may be important for dogs and rodents)

Biochemical interactions and metabolic products

Presence of gaseous co-pollutants

Changes in exposure level (e.g. spikes in air-pollutant concentrations)

History of exposure (e.g. producing sensitization and/or adaptation)

959

960

961

962 Table 2. Computed particle deposition enhancement factors (DEFs) vs. square patch dimension and
 963 particle diameter for unit specific gravity spheres.
 964

DEF			
Particle Diam. (μm)	Patch size (mm)		
	0.1	1.0	3.0
0.01	52	18	6.7
0.1	58	18	7.1
1.0	81	20	6.9
10.0	113	42	22

965 Data from Balásházy et al. (1999).
 966
 967
 968

969 Table 3. Computational fluid dynamics modeled hot spot deposition enhancement factors (DEF) for an
 970 adult male at resting (5 L/min) and exercising (30 L/min) ventilation states. Source: Phalen
 971 et al. (2010).

Particle aerodynamic diameter (μm)	Ventilation (l/min)	DEF
1	5	107
2	5	110
5	5	115
1	30	80
2	30	190
5	30	380

972 Data from Balashazy et al. (2003).
 973

974 Figure Captions.

975 Figure 1a. Diagrammatic representation of respiratory tract regions in humans. Structures are anterior
976 nasal passages, ET1; oral airway and posterior nasal passages, ET2; bronchial airways, BB;
977 bronchioles, bb; and alveolar interstitial, AI. Reproduced from EPA (2009)

978 Figure 1b. Human lung structure, tissue barrier structure. (a) Low magnification of human lung tissue,
979 showing gas exchange parenchyma (GP), blood vessels (BV), and airways (AW); magnification
980 x15. Courtesy of the Institute for Anatomy, University of Bern, Bern, Switzerland. (b) Low
981 magnification scanning electron micrograph of gas exchange parenchyma, clearly showing alveoli
982 (A); magnification x60. (c) Higher magnification scanning electron micrograph of alveolar duct
983 (AD) with concentrically arranged alveoli (A) around it; magnification x180. Modified from Gehr et
984 al. (1978). (d) Scanning electron micrograph of broken up interalveolar septum showing
985 erythrocytes (EC) in a capillary and the air–blood tissue barrier (AT); A, alveoli; magnification
986 x550. Modified from Gehr et al. (1978). (e) Low magnification transmission electron micrograph of
987 interalveolar septa, with capillaries containing erythrocytes (black) meandering around a
988 connective tissue frame; A, alveolar air; magnification x500. Modified from Gehr et al. (1978). (f)
989 Higher magnification transmission electron micrograph of a capillary (C) with erythrocytes (black)
990 in an interalveolar septum; the three layers of the air–blood tissue barrier (AT) can be recognized;
991 A, alveolar air; magnification x4500. Picture sequence a-f from Chang et al. (2010), original
992 source, Zhang et al. (2005). Reprinted from Journal of Aerosol Science, 36(2), Zhang et al. 2005,
993 Copyright (2005), with permission from Elsevier.

994 Figure 2a. Comparison of total and regional deposition results from the ICRP and MPPD models for a
995 resting breathing pattern ($VT = 625 \text{ mL}$, $f = 12 \text{ min}^{-1}$) and corrected for particle inhalability.
996 Regions are extrathoracic, ET; tracheobronchial, TB; and alveolar, A. Panels a-b are for nose
997 breathing; panels c-d are for mouth breathing. (Reproduced from EPA 2009a, Chapter 4)

998 Figure 2b. Comparison of total and regional deposition results from the ICRP and MPPD models for a
999 light exercise breathing pattern ($VT = 1250 \text{ mL}$, $f = 20 \text{ min}^{-1}$) and corrected for particle
1000 inhalability. Regions are extrathoracic, ET; tracheobronchial, TB; and alveolar, A. Panels a-b are
1001 for nose breathing; panels c-d are for mouth breathing. (Reproduced from EPA 2009a, Chapter 4)

1002 Figure 3. Intake Fraction ranges for various release scenarios. Ranges for PM_{2.5} from power plants and
1003 industrial sources for various regions and countries are listed, with median values indicated, as
1004 well as from a hypothetical distributed energy power plant (DE) (Tainio et al. 2009; Levy et al.
1005 2009; Hao et al. 2007; Heath et al. 2006; Li and Hao 2003; Wang et al. 2006). Ranges for mobile
1006 source emissions of PM_{2.5} in the US and Mexico are included, as well as point values for NY
1007 street canyons and Hong Kong (Greco et al. 2007a; Zhou and Levy 2008; Greco et al. 2007b;
1008 Luo et al. 2010; Stevens et al. 2007). A range of indoor *iF* values for PM_{2.5} from smoking

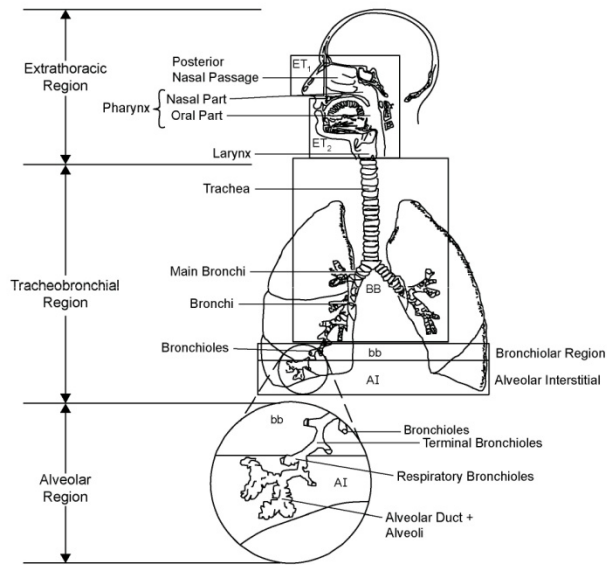
1009 sources is included (Klepeis and Nazaroff 2006). Values resulting from school buses and wood
1010 smoke are also included (Marshall and Behrentz 2005; Ries et al. 2009), as well as for a range of
1011 VOCs and SVOCs from outdoor emissions (Bennett et al. 2002b).

1012 Figure 4. Comparisons of micron- and nanoparticle deposition in an idealized upper airway model
1013 (Kleinstreuer and Zhang 2010). DEF, deposition enhancement factor. Reprinted from Annual
1014 Review Of Fluid Mechanics, 42, Kleinstreuer and Zhang 2010), Copyright (2010), with permission
1015 from Annual Reviews.

1016 Figure 5. Quantitative analyses of translocation of deposited UF particles from the air into the capillary
1017 blood in alveoli. (a) Illustration of the observed (white columns) and the expected (black columns)
1018 UF particles within the four tissue compartments which were analyzed at 1 h after exposure, (b)
1019 24 hours after exposure. The total chi-squared showed that the distributions of observed and
1020 expected particles differed significantly. There is only one compartment with an RDI > 1 and a
1021 substantial contribution to the total chi squared: the connective tissue is the only compartment
1022 that is preferentially targeted by the UF particles at 1 h after exposure and the capillary lumen is
1023 the only compartment that is preferentially targeted at 24 h after exposure respectively. Figures
1024 reproduced from Mühlfeld et al. (2007). Reproduced with permission from Particle and Fibre
1025 Toxicology 2007 per open access license.

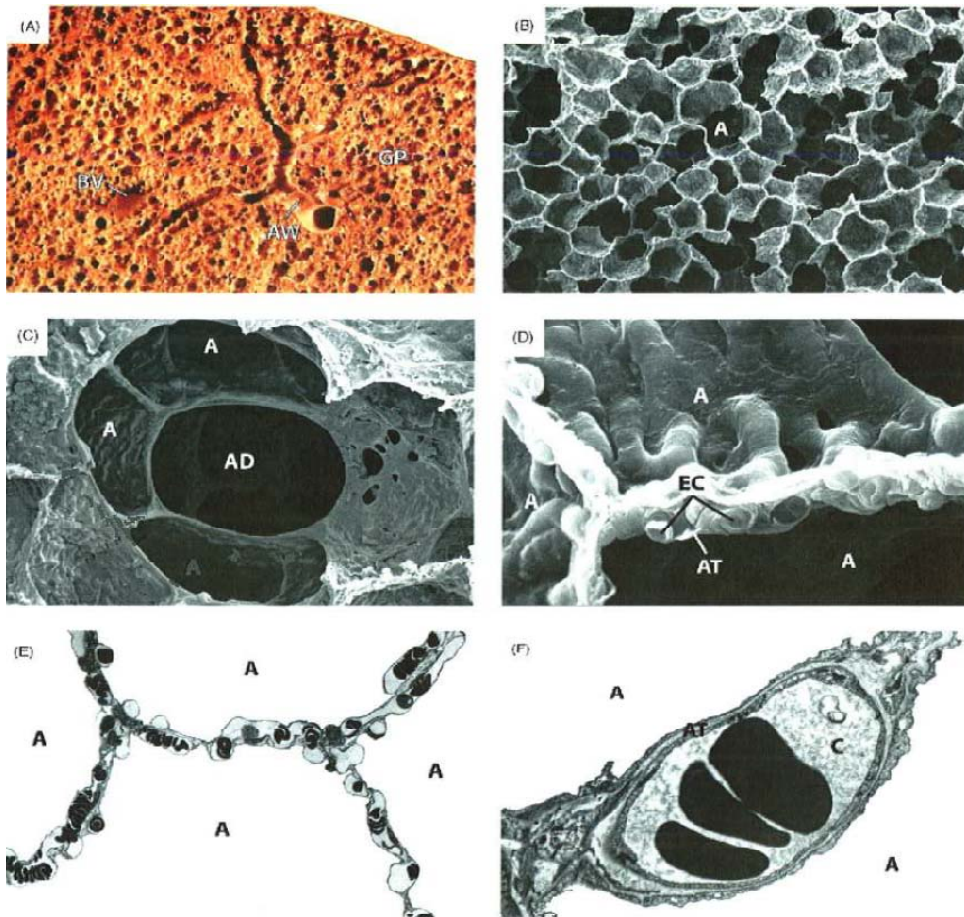
1026 Figure 6. A 549 epithelial cells (cell line) with gold UF particles (A, plain gold) and (B, PEG-coated gold).
1027 In (A), the particles (arrows) are localized within vesicles of different sizes, in (B) within a
1028 lysosome (arrows I) and in the cytosol (arrow II); n: nucleus, m: mitochondria; scale bars: 500 nm.
1029 Pictures from Brandenberger et al. (2010). Reprinted from Small, 6(15), Brandenberger et al.
1030 (2010), John Wiley and Sons, Copyright © 2010 Wiley-VCH Verlag GmbH & Co.

1031



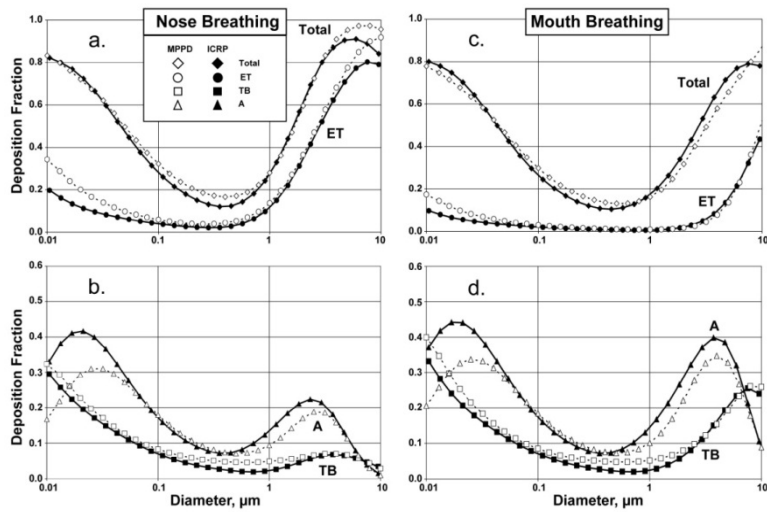
1032
1033
1034
1035
1036

Figure 1a.



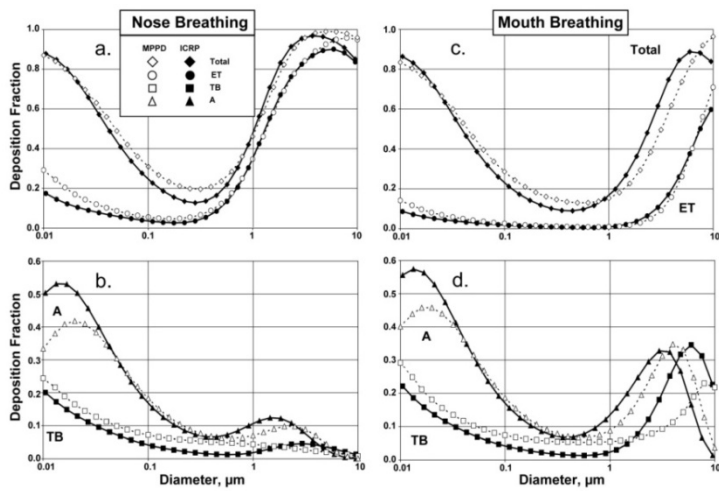
1037
1038
1039

Figure 1b.



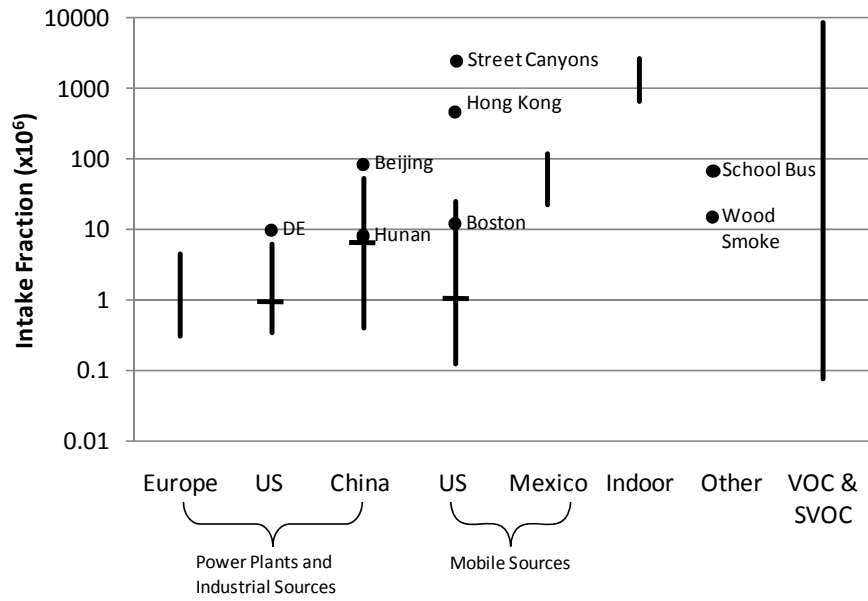
1040
1041
1042
1043

Figure 2a.



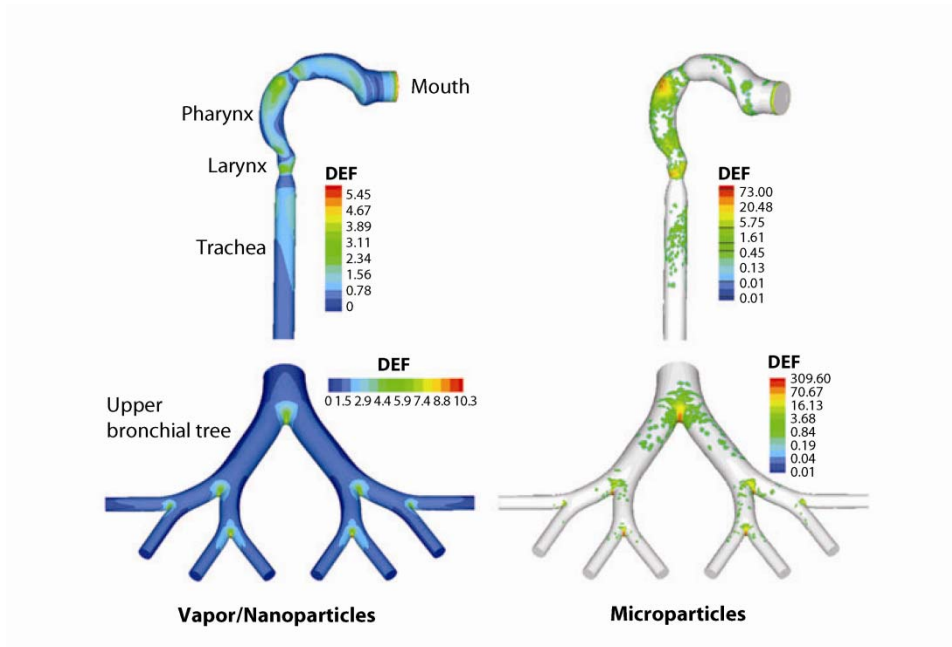
1044
1045
1046
1047
1048

Figure 2b



1049
1050
1051
1052

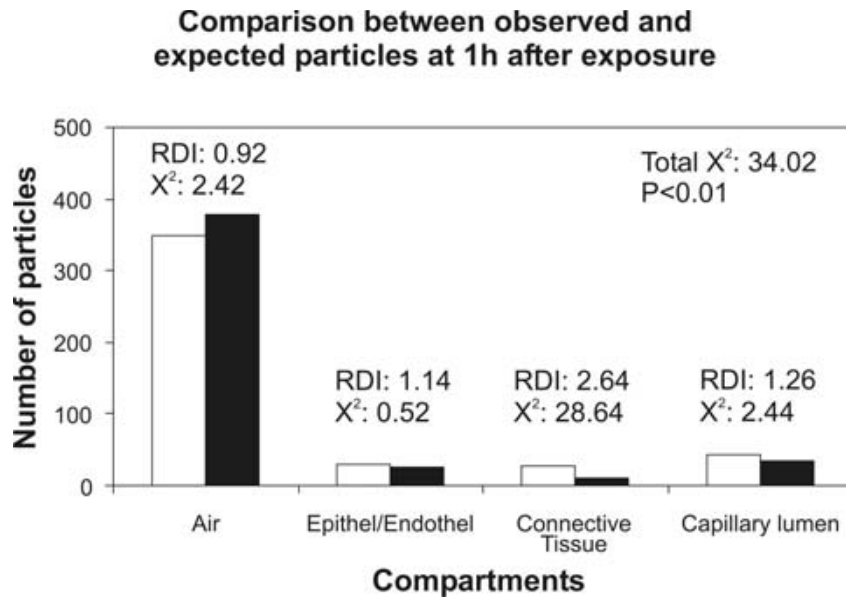
Figure 3.



1053
1054
1055
1056
1057
1058

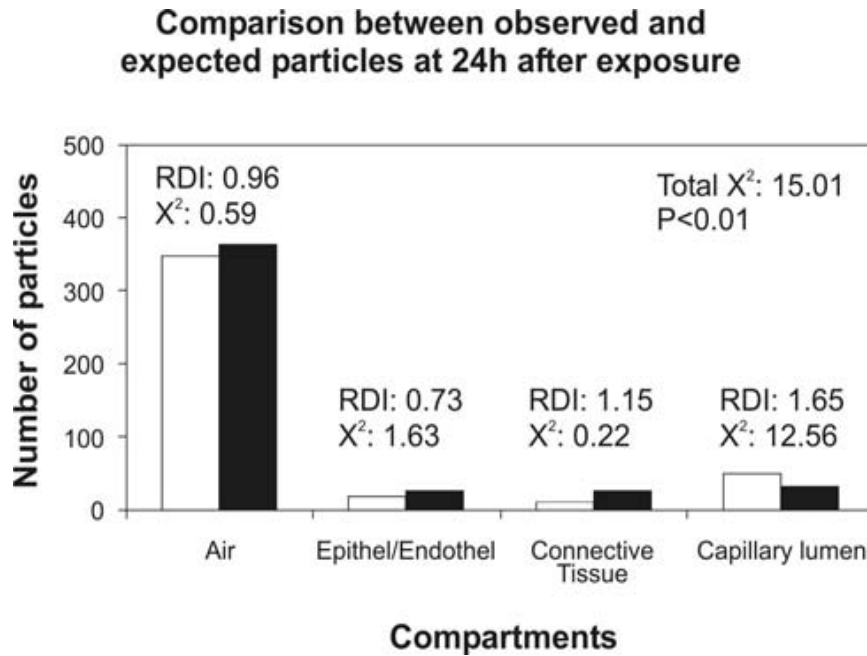
Figure 4.

1059
1060
1061



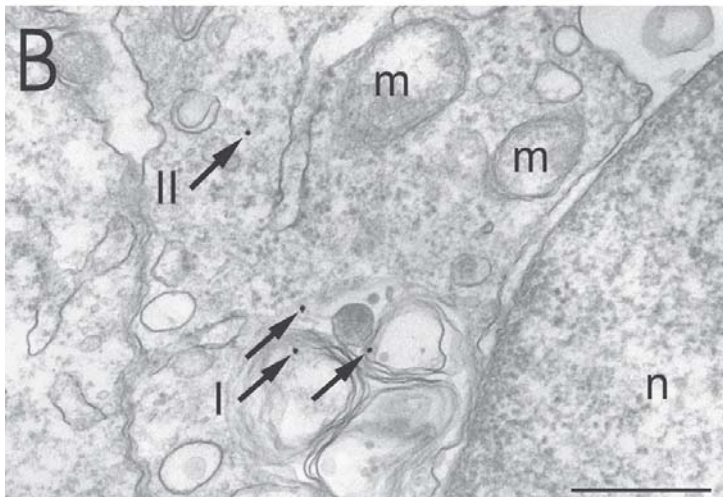
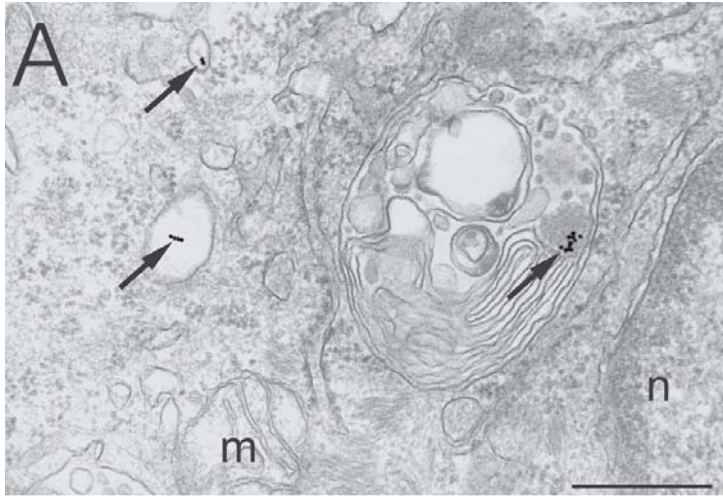
1062
1063
1064
1065
1066

Figure 5a.



1067
1068
1069

Figure 5b.



1070
1071
1072

Figure 6.